OPEN ACCESS

Original research

Suppressor CD4$^+$ T cells expressing HLA-G are expanded in the peripheral blood from patients with acute decompensation of cirrhosis

Wafa Khamri ,[1] Cathrin Gudd,[1] Tong Liu,[1] Rooshi Nathwani ,[1] Marigona Krasniqi,[1] Sofia Azam,[1] Thomas Barbera,[1] Francesca M Trovato,[2] Lucia Possamai,[1] Evangelos Triantafyllou ,[1] Rocio Castro Seoane,[1] Fanny Lebosse,[1] Arjuna Singanayagam,[1] Naveenta Kumar,[1] Christine Bernsmeier,[1,2] Sujit Mukherjee,[1] Mark McPhail ,[2] Chris J Weston,[3] Charalambos Gustav Antoniades,[1] Mark R Thursz[1]

ABSTRACT

Objective Identifying components of immuneparesis, a hallmark of chronic liver failure, is crucial for our understanding of complications in cirrhosis. Various suppressor CD4$^+$ T cells have been established as potent inhibitors of systemic immune activation. Here, we establish the presence, regulation and mechanism of action of a suppressive CD4$^+$ T cell subset expressing human leucocyte antigen G (HLA-G) in patients with acute decompensation of cirrhosis (AD).

Design Flow cytometry was used to determine the proportion and immunophenotype of CD4$^+$HLA-G$^+$ T cells from peripheral blood of 20 healthy controls (HCs) and 98 patients with cirrhosis (28 with stable cirrhosis (SC), 20 with chronic decompensated cirrhosis (CD) and 50 with AD). Transcriptional and functional signatures of cell-sorted CD4$^+$HLA-G$^+$ cells were delineated by NanoString technology and suppression assays, respectively. The role of immunosuppressive cytokine interleukin (IL)-35 in inducing this population was investigated through in vitro blockade experiments. Immunohistochemistry (IHC) and cultures of primary human Kupffer cells (KCs) were performed to assess cellular sources of IL-35. HLA-G-mediated T cell suppression was explored using neutralising antibodies targeting co-inhibitory pathways.

Results Patients with AD were distinguished by an expansion of a CD4$^+$HLA-G$^+$CTLA-4$^+$IL-35$^+$ immunosuppressive population associated with disease severity, clinical course of AD, infectious complications and poor outcome. Transcriptomic analyses excluded the possibility that these were thymic-derived regulatory T cells. IHC analyses and in vitro cultures demonstrate that KCs represent a potent source of IL-35 which can induce the observed HLA-G$^+$ phenotype. These exert cytotoxic T lymphocyte antigen-4-mediated impaired responses in T cells paralleled by an HLA-G-driven downregulation of T helper 17-related cytokines.

Conclusion We have identified a cytokine-driven peripherally derived suppressive population that may contribute to immuneparesis in AD.

Significance of this study

What is already known on this subject?

- Disturbed peripheral immune mechanisms and susceptibility to developing infections are common features of acute decompensation of cirrhosis (AD).
- Despite advances in understanding various mechanisms of innate immune dysfunction leading to infectious complications in cirrhosis, dysregulation of the adaptive arm of the immune system remain partially explored.
- Several subsets of regulatory T cells have been shown to play an important role in T cell-mediated suppression in immune dysregulated diseases.
- Here, we assess the presence and the role of novel regulatory CD4$^+$HLA-G$^+$ T cells in failure to mount effective immune responses in AD.

What are the new findings?

- Expansion of non-classical regulatory CD4$^+$HLA-G$^+$ T cells which are (1) induced by lipopolysaccharide-driven immunosuppressive cytokine interleukin-35 from Kupffer cells (2) suppressive to T cells functions through a cytotoxic T lymphocyte antigen-4-dependent pathway and displays an human leucocyte antigen G (HLA-G)-mediated attenuation of T helper 17-related cytokines (3) associated with complications in cirrhosis.
- We provide novel insights into identifying key targeted immunotherapy-based strategies to restore pivotal immune responses and improve patient outcomes.

How might it impact on clinical practice in the foreseeable future?

- This study provides novel cellular and mechanistic insights into defective peripheral immune responses in AD.
- This is essential to understanding pathophysiology of immune dysfunctions in AD and exploiting potential biomarkers, predictors of AD clinical progression and therapeutic targets in reversing immunosuppression in these patients.

► Additional supplemental material is published online only. To view, please visit the journal online (http://dx.doi.org/10.1136/gutjnl-2021-324071).

[1]Section of Hepatology & Gastroenterology, Division of Digestive Diseases, Department of Metabolism, Digestion & Reproduction, Imperial College London, London, UK
[2]Department of Inflammation Biology, Institute of Liver Studies, King's College London, London, UK
[3]NIHR Biomedical Research Unit and Centre for Liver Research, University of Birmingham, Birmingham, UK

Correspondence to
Dr Wafa Khamri, Section of Hepatology & Gastroenterology, Division of Digestive Diseases, Department of Metabolism, Digestion & Reproduction, Imperial College London, London, UK;
w.khamri@imperial.ac.uk

Received 8 January 2021
Accepted 22 July 2021
Published Online First 3 August 2021

Check for updates

© Author(s) (or their employer(s)) 2022. Re-use permitted under CC BY. Published by BMJ.

To cite: Khamri W, Gudd C, Liu T, *et al*. *Gut* 2022;**71**:1192–1202.

Gut: first published as 10.1136/gutjnl-2021-324071 on 3 August 2021. Downloaded from http://gut.bmj.com/ on April 17, 2024 by guest. Protected by copyright.

INTRODUCTION

Cirrhosis is a progressive disease of the liver characterised by diffuse fibrosis, disruption of intrahepatic venous flow and portal hypertension, which may progress to liver failure.[1 2] It is categorised into asymptomatic stable cirrhosis (SC) and symptomatic acutely decompensated cirrhosis (AD). Decompensation defines patients with a failure in liver synthetic function (jaundice) or the development of complications related to their cirrhosis and portal hypertension, such as variceal bleeding, ascites or hepatic encephalopathy. Patients with AD can present without or with acute-on-chronic-liver failure (ACLF), a syndrome characterised by extrahepatic organ failure and high short-term mortality[3] (AD-No ACLF and AD-ACLF, respectively).[4 5] A progressive dysfunctional immune response, referred to as cirrhosis-associated immune dysfunction, arising from persistent or episodic systemic inflammation together with defects in immune response to microbial cues, termed immuneparesis, represents a key component of the pathogenesis of cirrhosis. Independent of cirrhosis stage and aetiology, these alterations in immune responses engender a marked susceptibility to infections, estimated to occur in 35%–45% of hospitalised patients. In particular, the development of immuneparesis is associated with infectious complications in cirrhosis.[6–9] Thus far, the contribution of defects in innate monocyte/macrophage-mediated immune responses to immuneparesis has been well studied and proven to be an important contributor to impaired antimicrobial responses in these patients.[8 10–14] Exploring implications of dysfunctions in adaptive host immunity in the pathophysiology of cirrhosis is an increasing focus of research. Indeed, we recently made progress in understanding the impact of adaptive immune defects in systemic immunity in cirrhosis by showing dysfunction in the $CD8^+$ T cell population, with an expansion of a suppressor peripheral $CD8^+$ T cell populations in patients with cirrhosis, characterised by high human leucocyte antigen (HLA)-DR and TIM-3 surface expression, associated with concomitant infections and disease severity, respectively.[15] We therefore suggest a key role of suppressive regulation as a mediator of impairment of systemic adaptive immune responses in patients with liver disease.

It is well known that dysregulation in immune responsiveness can be governed by several mechanisms including suppression of immune activation through regulatory T cells (Tregs).[16–18] Multiple subsets of Tregs with specialised activities have been described to suppress antimicrobial responses. The best characterised Tregs feature in the $CD4^+$ T cell subset. Besides the major population of suppressor $CD4^+CD25^+CD127^{low}$ Tregs (termed thymus-derived Tregs (tTregs)), novel peripherally derived regulatory $CD4^+$ T cells have been described.[19] Identified based on surface expression of HLA-G, a non-classical HLA class I tolerogenic molecule, $CD4^+$HLA-G^+ T cells have been described to dampen the extent of an immune response and play a role in tissue tolerance.[20–24] They were reported to inhibit allogeneic responses, induce regulatory cells, inhibit the functions of natural killer (NK) cells and cytotoxic T lymphocytes, upregulate inhibitory receptor expression and inhibit dendritic cell maturation.[25 26] HLA-G expressing $CD4^+$ T cells were further characterised by the expression of interleukin (IL)-35, a potent anti-inflammatory cytokine linked to suppression of T cell function.[27–29] In this study, we identify a T cell population with potential contribution to unbalanced immune responses in AD in the expansion of an IL-35-induced $CD4^+$HLA-G^+ T cells displaying a cytotoxic T lymphocyte antigen-4 (CTLA-4)-dependent suppressive capacity of T cell functions and an HLA-G-mediated downregulation of cytokines required for a T helper 17 (Th17) pro-inflammatory immune response.

MATERIALS AND METHODS

Patient characteristics

Ninety-eight patients with cirrhosis were included in this study and categorised into: ambulatory patients with SC (n=28), chronic decompensated cirrhosis (CD, n=20, including both 'unstable decompensated cirrhosis' requiring readmission and 'stable decompensated cirrhosis' admitted only for elective procedures (as per definition of PREDICT study))[5] and patients with acute decompensation of cirrhosis (AD, n=50) (defined as patients who presented to hospital with acute decompensation±organ failure (25 (AD without organ failure (AD-No ALCF) and 25 with organ failure (AD-ACLF)). Their clinical and biological parameters are presented in table 1. Patients were recruited from February 2016 to December 2020. Cirrhosis was diagnosed by a combination of clinical examination, laboratory and radiological information, and histology where available. Detailed patient criteria are described in online supplemental methods. Twenty healthy volunteers served as healthy controls (HCs).

Phenotyping and intracellular cytokine staining using flow cytometry

Cell surface and intracellular cytokine staining of peripheral blood mononuclear cells (PBMCs) were carried out using fluorochrome-labelled monoclonal antibodies (online supplemental table S1), as detailed in online supplemental methods.

Cell sorting and NanoString gene expression profiling

Using FACS Aria II flow cytometer (Becton Dickinson, Oxford, UK), viable $CD3^+CD8^-CD4^+$ T cells from patients with AD (AD-ACLF, n=4) were subject to a three-way sort (gating strategy in online supplemental figure S1A). NanoString nCounter GX Human Immunology V2 assay (NanoString Technologies, Seattle, Washington, USA) was carried out as described in online supplemental methods.

HLA-G^+ cell isolation using magnetic bead cell separation

$CD4^+$ T cells were isolated from PBMCs by negative selection using magnetic-activated cell sorting (MACS) microbeads (Miltenyi Biotec, Surrey, UK) according to manufacturer's instructions. Purified $CD4^+$ T cells from patients with AD (AD-ACLF, n=3) were then stained with FITC-conjugated anti-HLA-G monoclonal antibody (clone MEM-G/9) (Invitrogen, Carlsbad, USA) for 25 min at 4°C. Fluorescein isothiocyanate (FITC)-labelled HLA-G^+ T cells were then washed, incubated with anti-FITC microbeads (Miltenyi Biotec), then positively selected following manufacturer's protocol. Gene expression levels of HLA-G mRNA were assessed in the isolated $CD4^+$ cells and compared with the $CD4^-$ fraction as detailed in the online supplemental methods.

Suppression assays

Bead-isolated $CD4^+$HLA-G^+ T cells from patients with AD (AD-ACLF, n=3) were tested for their suppressive capacities in co-cultures with allogeneic PBMCs isolated from HCs. Prior to co-culture, allogeneic PBMCs were stained with 10 μM cell proliferation dye (CPD) eFluor 670 (eBioscience, Hatfield, UK) as per manufacturer's protocol. Cells were cultured at different responder:HLA-G^+ suppressor ratios (16:1, 8:1, 4:1 and 2:1) in TexMACS serum-free medium (Miltenyi Biotec) in the presence of anti-CD3 monoclonal antibody stimulation (α-CD3, 0.5 μg/mL) (eBioscience) for 5 days at 37°C in 5% CO_2. Proliferation was then measured on gated $CD3^+$ T cells by dilution of the CPD-eFluor 670 dye

Gut: first published as 10.1136/gutjnl-2021-324071 on 3 August 2021. Downloaded from http://gut.bmj.com/ on April 17, 2024 by guest. Protected by copyright.

Table 1 Demographics and clinical parameters of patients with SC, CD and AD and HCs

Parameter	HCs (n=20)	SC (n=28)	CD (n=20)	AD (n=50)
Age—years	38.00 (32.00–50.50)	58.00† (49.50–63.50)	55.50† (47.25–62.00)	49.50 (42.00–58.00)
Gender—n (%)				
Male	14/20 (70%)	21/28 (75%)	14/20 (70%)	37/50 (74%)
Female	6/20 (30%)	7/28 (25%)	6/20 (30%)	13/50 (26%)
Aetiology—n (%)				
Alcoholic liver disease (ALD)	NA	19/28 (67.8%)	12/20 (60%)	32/50 (64%)
Hepatitis C**	NA	2/28 (7.14%)	–	3/50 (6%)
Hepatitis C+ALD	NA	–	–	1/50 (2%)
Autoimmune hepatitis	NA	–	2/20 (10%)	2/50 (4%)
NAFLD	NA	3/28 (10.7%)	–	6/50 (12%)
Cryptogenic	NA	3/28 (10.7%)	–	3/50 (6%)
Other††	NA	1/28 (3.5%)	6/20 (30%)	3/50 (6%)
White cell count—$\times10^9$/L	NA	4.65‡*** (3.75–6.03)	4.415§*** (2.648–6.155)	8.52‡***§*** (6.30–15.14)
Neutrophils—$\times10^9$/L	NA	2.92‡*** (2.10–4.20)	2.50§*** (1.88–4.01)	6.20‡***§*** (3.78–10.52)
Monocytes—$\times10^9$/L	NA	0.410‡*** (0.30–0.60)	0.33§*** (0.21–0.487)	0.87‡***§*** (0.47–1.20)
Lymphocytes—$\times10^9$/L	NA	1.19 (0.82–1.61)	0.93 (0.70–1.41)	1.10 (1.57–0.61)
MELD score	NA	10.90‡***¶* (7.85–15.68)	16.53¶* (10.92–23.13)	26.10‡*** (15.8–33.00)
SOFA score (CLIF-SOFA score in ACLF)	NA	NA	3.50§*** (3.00–4.00)	12.00§*** (8.50–14.50)
CLIF AD score (in AD) CLIF ACLF (in ACLF)	NA	NA	NA	54.50 (45.75–62.13) 58.90 (52.00–64.10)
Child-Pugh score	NA	8.00‡*** (6.00–9.00)	8.50§** (7.00–10.00)	11.00‡***§** (9.00–12.00)
Creatinine—µmol/L	NA	72.00¶*** (57.75–88.75)	66.50§***¶*** (54.00–88.75)	78.50*** (58.5–131.8)
Bilirubin—µmol/L	NA	26.5¶*** (16.50–50.25)	2.54§***¶*** (1.50–7.58)	59.00§*** (26.0–154.0)
CRP—mg/L	NA	5.05‡*** (2.40–15.58)	13.60§*** (6.60–17.80)	33.80‡***§*** (16.90–68.00)
INR	NA	1.28‡*** (1.10–1.60)	1.36§* (1.190–1.783)	1.72‡***§* (1.46–2.02)
Ammonia—µmol/L	NA	ND	56.00§*** (46.00–111.0)	133.80§*** (126.0–136.0)
Type of precipitating events—n (%)‡‡				
GI bleed				19 (38%)
Infection				13 (26%)
Acute alcohol injury	NA	NA	NA	3 (6%)
Any of the events in combination				7 (14%)
Unknown				8 (16%)
Number of precipitating events—n (%)				
1				35 (70%)
≥2				7 (14%)
Mortality from enrolment—n (%)	NA	NA	NA	24 (48%)
90-day mortality				

Values represent medians (IQR) unless otherwise stated.
Multiple comparison testing between more than two groups was carried out using Kruskal-Wallis test with Dunn's test post hoc intergroup comparison. Mann-Whitney U test used for comparison between two groups.
*P<0.0005 and ***p<0.0001.
†Significant differences in age compared with HCs, p=0.0005.
‡Comparison between AD and SC.
§Comparison between AD and CD.
¶Comparison between SC and CD.
**Treated hepatitis C.
††Other aetiologies include Wilson's disease, Alagille syndrome, chronic Budd-Chiari syndrome and primary sclerosing cholangitis.
‡‡Numbers and percentages presented are in GI bleed alone versus infection alone versus acute alcohol injury alone. Seven patients (14%) had more than one type of event (three patients presented with infection and GI bleed/two with acute alcohol injury and infection, one with GI bleed and acute alcohol injury and one with the three precipitating events).
ACLF, acute-on-chronic-liver failure; AD, acute decompensation of cirrhosis; CD, chronic decompensated cirrhosis; CLIF-SOFA, chronic liver failure-sequential organ failure assessment; CRP, C reactive protein; HCs, healthy controls; INR, international normalised ratio; MELD, model for end-stage liver disease; NA, not applicable; NAFLD, non-alcoholic fatty liver disease; ND, not determined; SC, stable cirrhosis.

using flow cytometry. Suppressive capacity was measured as percentage of suppression calculated as: [100−(% proliferation of responders:suppressors/% proliferation of responders only)×100].[30]

Measurement of IL-35 in sera samples and cell culture supernatants using ELISA

Concentrations of IL-35 in human sera samples or supernatants collected from cultured cells were measured using ELISA (Elabscience, Bethesda, MD, USA), according to manufacturer's instructions. The optical density was measured at 450 nm using the Multiskan Go plate reader (Thermo Fisher Scientific, Hemel Hempstead, UK).

Sera conditioning of isolated CD4$^+$ T cells

CD4$^+$ T cells were seeded at 2.5×10^5 cells/well on 24-well plates (Starlab, Milton Keynes, UK) and cultured for 48 hours in the presence of 25% sera derived from patients or HCs (n=15 per group). The effect of IL-35 present in the sera (n=12) on driving an HLA-G-positive phenotype was tested through sera pretreatment with

Gut: first published as 10.1136/gutjnl-2021-324071 on 3 August 2021. Downloaded from http://gut.bmj.com/ on April 17, 2024 by guest. Protected by copyright.

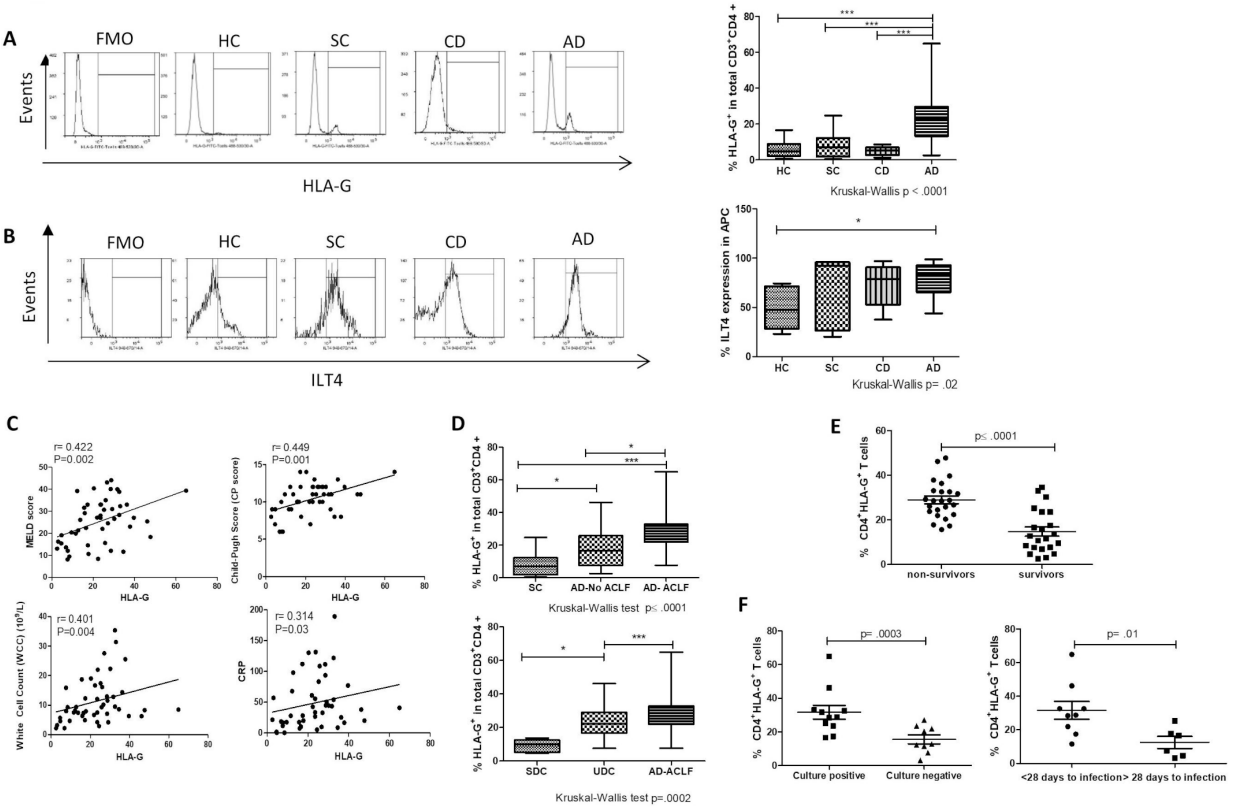

Figure 1 Expansion of $CD4^+HLA\text{-}G^+$ T cell population in patients with acute decompensation of cirrhosis (AD). Peripheral blood mononuclear cells (PBMCs) from healthy controls (HCs) (n=20) and patients (stable cirrhosis (SC), n=28; chronic decompensated cirrhosis (CD), n=20 and AD, n=50) were assessed for surface levels of human leucocyte antigen G (HLA-G) using flow cytometry (gating strategy online supplemental figure S1A). (A) Representative flow cytometry histograms used to determine HLA-G levels, all gated based on fluorescence-minus-one (FMO) controls (left panel). Percentage of HLA-G expressing cells in $CD3^+CD4^+CD8^-$T cells in HCs compared with patients with SC, CD and AD (right panel). (B) Representative histograms of immunoglobulin-like transcript 4 (ILT4) levels on monocytes in HCs and patients (SC, CD and AD) (left panel). Distribution of $ILT4^+$ monocytes in HCs and in patients (right panel). (C) Correlation of the frequency of $CD4^+HLA\text{-}G^+$ T cells with clinical parameters and disease severity scores in patients with AD (model for end-stage liver disease (MELD) scores, Child-Pugh (CP), white cell count (WCC) and C reactive protein (CRP)). (D) Distribution of $CD4^+HLA\text{-}G^+$ T cells with increasing disease severity in patients within the AD cohort (AD-No ACLF, n=25; AD-acute-on-chronic-liver failure (ACLF), n=25) compared with SC (n=28) (top panel). Distribution of $CD4^+HLA\text{-}G^+$ T cells across the clinical phenotypes of AD (stable decompensated cirrhosis (SDC), n=8; unstable decompensated cirrhosis (UDC), n=13) and AD-ACLF (n=25) (no analyses of the pre-ACLF were performed due to the limited number of this phenotype in the patient cohort) (bottom panel). (E) Distribution of $CD4^+HLA\text{-}G^+$ T cells in non-surviving (n=24) and surviving patients (n=23) with AD within 90 days following admission. (F) HLA-G expression was assessed in patients with AD who developed culture-positive primary infections (n=11) and the ones who developed culture-negative infections (n=9) (left panel). Distribution of $HLA\text{-}G^+$ T cells was compared in patients withh AD who developed short-term secondary infections (n=9) (<28 days) and the ones who developed it in >28 days (n=6) (right panel). Non-parametric statistical analysis was used (Mann-Whitney U test for two group comparison and Kruskal-Wallis followed by a Dunn's test for multiple comparisons between more than two groups). Data are presented as median values with IQR. Correlation coefficients (r) and correlation p values were tested using non-parametric Spearman's correlation test. *P<0.05; ***p<0.0005.

0.5 µg/mL anti-IL-35 neutralising antibody (α-IL-35) (Bio-Techne, Abingdon, UK) prior to culture isolated $CD4^+$ T cells for 45 min at room temperature. Similarly, controls were carried out in the presence or absence of anti-IL-10 neutralising antibody (α-IL-10, at 1 µg/mL) (Bio-Techne). The phenotype of the cells following sera conditioning was screened using flow cytometry.

Immunohistochemistry

Immunohistochemistry (IHC) of liver explants obtained from liver transplantation of patient with AD with ACLF and patient with SC was carried out as depicted in online supplemental methods.

Primary human Kupffer cell cultures

Cryopreserved Kupffer cells (KCs) (Thermo Fisher Scientific) were stimulated for 48 hours in the presence of 100 ng/mL *Escherichia coli* lipopolysaccharide (LPS) (Sigma-Aldrich, Dorset, UK) or human high mobility group box 1 (HMGB1) (R&D Systems, Abingdon, UK). Prior to LPS or HMGB1 stimulation, KCs were treated with or without blocking antibodies against toll-like receptor 4 (α-TLR4) or CD14 as detailed in the online supplemental methods. Cell culture supernatants were collected for assessment of IL-35 concentrations using ELISA.

Proliferation assays and multiplex cytokine detection system

Following 48-hour sera treatment, $CD4^+HLA\text{-}G^+$ generated in response to AD sera were collected and incubation with carboxyfluorescein succinimidyl ester-labelled PBMCs and α-CD3 stimulation (0.5 µg/mL) (eBioscience) in the presence or absence of either α-CTLA-4 (10 µg/mL) (eBioscience), α-HLA-G (10 µg/mL) (Miltenyi Biotec) or α-IL-35 (0.5 µg/mL) (Bio-Techne, Abingdon, UK) neutralising antibodies. Cells were co-cultured for 5 days to allow measurement of proliferation in $CD3^+$ responder T cells.

Gut: first published as 10.1136/gutjnl-2021-324071 on 3 August 2021. Downloaded from http://gut.bmj.com/ on April 17, 2024 by guest. Protected by copyright.

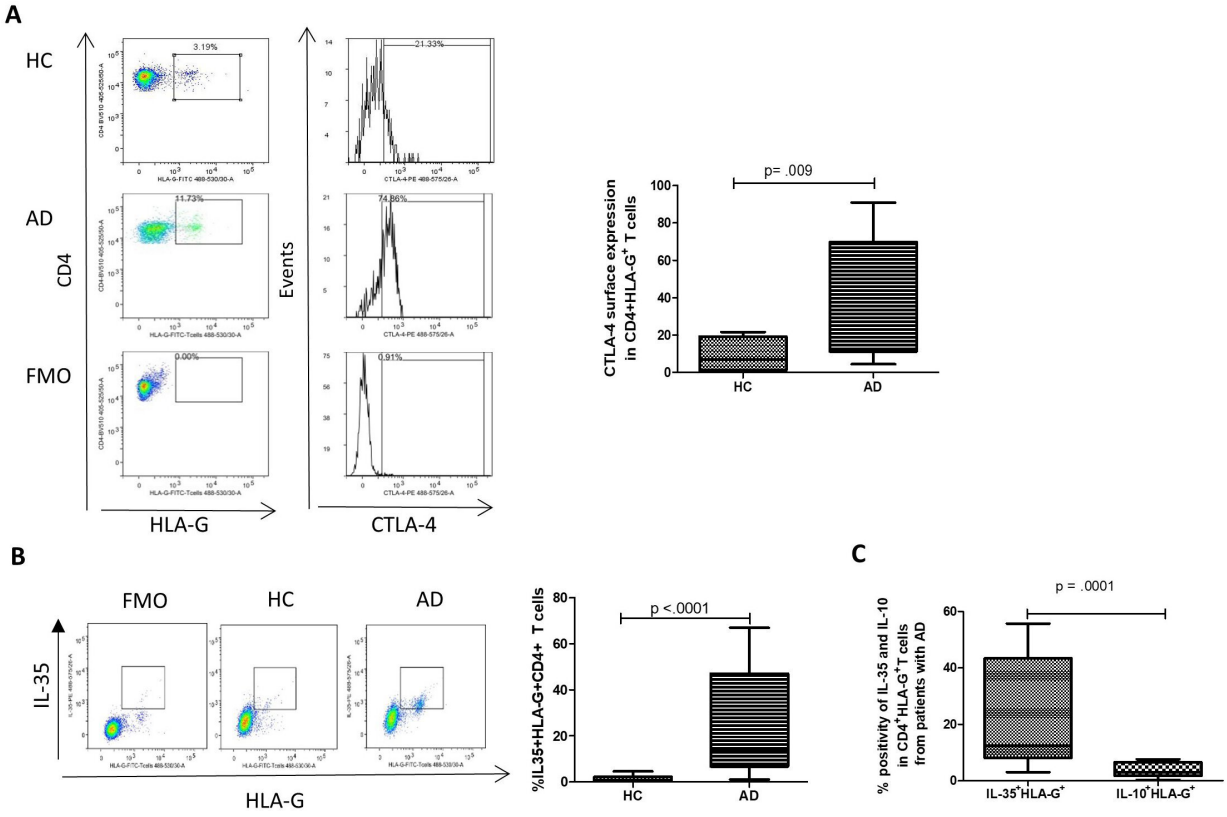

Figure 2 Immunophenotyping to characterise $CD4^+HLA\text{-}G^+$ population in patients with acute decompensation of cirrhosis (AD) demonstrates that the population is $CTLA\text{-}4^{high}IL35^{high}IL\text{-}10^{low}$. (A) Representative flow dot plots and histograms of surface levels of inhibitory marker CTLA-4 assessed in $CD4^+HLA\text{-}G^+$ (left panel). CTLA-4 levels on $CD4^+HLA\text{-}G^+$ T cells in healthy controls (HCs) and in patients with AD (right panel). (B) Representative dot plots of intracellular cytokine staining used to define levels of interleukin (IL)-35 in the $CD4^+HLA\text{-}G^+$ population (left panel). Co-expression of HLA-G and IL-35 in HCs compared with patients with AD (right panel). (C) $CD4^+HLA\text{-}G^+$ T cells assessed for their co-expression of IL-35 and IL-10 in patients with AD (n=14). Mann-Whitney U test for two group comparison. Data are presented as median values with IQR. HLA-G, human leucocyte antigen G; CTLA-4, cytotoxic T lymphocyte antigen-4; FMO, fluorescence minus one.

Supernatants were collected to assess cytokine secretion in the T helper 1 (Th1)/T helper 2 and Th17 pathways using multiplex cytokine detection system (Meso Scale Discovery System, Rockville, USA) (see online supplemental methods).

Statistical analyses

Following assessment of normality for continuous data, the Mann-Whitney U test was used for non-parametric data and Wilcoxon matched pairs signed rank test was used for paired tests. Multiple comparison testing between more than two groups was carried out using Kruskal-Wallis test with Dunn's test post hoc intergroup comparison. Spearman's correlation coefficients were calculated for correlation analyses. Statistical significance was assumed for p values ≤ 0.05. Data analysis was performed using GraphPad Prism 5 (GraphPad Software, San Diego, California, USA).

RESULTS

Patient characteristics

Age and gender were similar in the pathological groups. When patients were compared with HCs, there were no differences in gender proportion. However, patients with SC and CD were older than HCs (table 1). The most common underlying disease in all patient groups was alcohol-related liver disease (ALD) (67.8%, 60% and 64% in SC, CD and AD, respectively). White cell count (WCC), creatinine, bilirubin, C reactive protein (CRP) and international normalised ratio (INR), and were all significantly elevated in patients with AD compared with SC and CD (table 1). Patients with AD had higher disease severity indices including Child-Pugh (CP) and model for end-stage liver disease (MELD) scores (table 1). GI bleed and infection were the main precipitating events (PE) of AD (38% and 26%, respectively) (table 1).

Increased proportion of circulating $CD4^+$ T cells exhibiting high levels of HLA-G in patients with AD

Phenotypic analyses to evaluate the expression of HLA-G on circulating $CD4^+$, $CD8^+$ T cells and monocytes from HCs, patients with SC and AD were carried out (gating strategies described in online supplemental figure S1B). Data revealed a distinct elevation of HLA-G expression within the $CD4^+$ T cell subset (figure 1A) but not $CD8^+$ T cells or monocytes where no detectable HLA-G expression was seen (online supplemental figure S1C). The expansion of the $CD4^+HLA\text{-}G^+$ population was markedly predominant in patients with AD compared with HCs, SC and CD (median 23.54%; IQR (13.28–29.69) vs 4.61%; (2.18–8.81) 7.09%; (1.83–12.25) and 5.14 (2.62–6.97)), respectively (Kruskal-Wallis $p<0.0001$) (figure 1A). Although there was some variation between patients, expression of HLA-G on the $CD4^+$ T cell subset was further confirmed at the transcriptional level (online supplemental figure S1D). While HCs were significantly younger than patients with SC and CD, proportions of $CD4^+HLA\text{-}G^+$ did not vary with age (online supplemental figure S1E). On the other hand, monocytes (defined as $HLA\text{-}DR^+CD14^+CD1a^-CD11c^+CD86^+$) from patients with AD

Gut: first published as 10.1136/gutjnl-2021-324071 on 3 August 2021. Downloaded from http://gut.bmj.com/ on April 17, 2024 by guest. Protected by copyright.

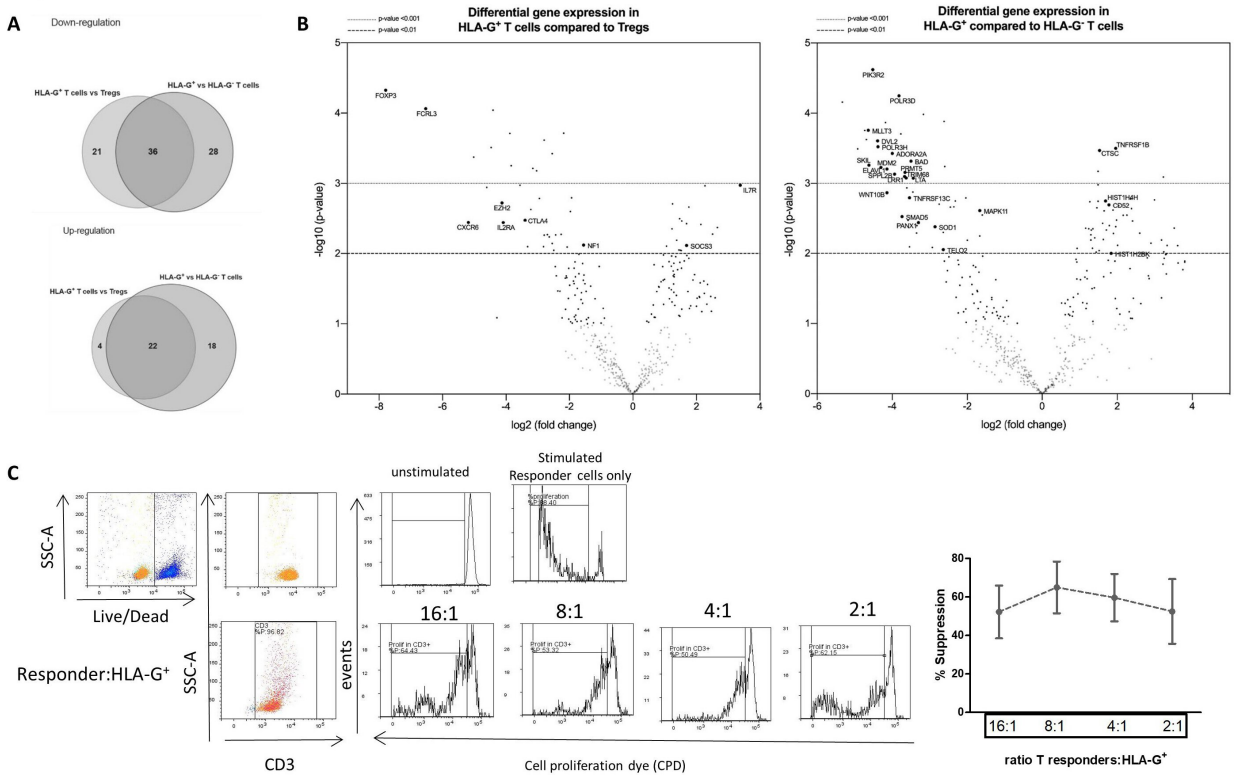

Figure 3 Transcriptional and functional features of CD4$^+$HLA-G$^+$ T cells from patients with acute decompensation of cirrhosis (AD). (A) Quantitative analysis of immune-related gene in HLA-G$^+$ compared to thymus-derived regulatory T cells (tTregs) and or HLA-G$^-$ counterparts from patients with AD (n=4) using NanoString Technologies. Data show Venn diagrams of significantly differentially expressed (DE) genes. (B) Volcano plots comparing HLA-G$^+$ T cells to either tTregs or HLA-G$^-$ T cells. Gene names are listed for DE genes showing that gene expression pattern of immune-related genes in circulating CD4$^+$HLA-G$^+$ T cells are distinct from Tregs and HLA-G-negative counterparts. (C) HLA-G$^+$ cells suppressive capacity on CPD-labelled responder peripheral blood mononuclear cells (PBMCs) proliferation. Representative histograms of live CD3$^+$ T cells proliferating in the absence or presence of α-CD3 stimulation (top left panel). Representative flow histograms of proliferating CD3$^+$ T cells in the presence of HLA-G$^+$ fractions at the tested ratios (bottom left panel). Suppressive capacity of HLA-G$^+$ (n=4) isolated from patients with AD after 5 days of co-culture (right panel). HLA-G, human leucocyte antigen G.

displayed elevated levels of immunoglobulin-like transcript 4 (ILT4), an HLA-G-associated receptor[25] (figure 1B).

Proportions of CD4$^+$HLA-G$^+$ T cells correlate with disease severity and poor outcome

In patients with AD, HLA-G expression on CD4$^+$ T cells correlated positively with MELD score (r=0.422, p=0.002), CP score (r=0.449, p=0.001), WCC (r=0.401, p=0.004) and CRP (r=0.314, p=0.03) (figure 1C). The correlations with disease severity scores were further corroborated by the increased frequency of the CD4$^+$HLA-G$^+$ population with increasing severity of disease (figure 1D). Among patients who died within 90 days of admission, the proportion of CD4$^+$HLA-G$^+$ T cells at baseline was significantly higher than in patients who survived (p≤0.0001) (figure 1E). Analyses among patients with AD with infectious complications revealed that percentage of HLA-G$^+$ cells was significantly elevated in patients with culture-positive primary infections compared with culture-negative ones (p=0.003) (figure 1F). Additionally, patients who later developed secondary infections in <28 days from hospital admission had increased frequency of HLA-G$^+$ cells (p=0.01) (figure 1F).

Distinct distribution of CD4$^+$HLA-G$^+$ T cells in different clinical courses of AD

In addition to the two distinct clinical presentations of AD depending on the absence or presence of organ failure (AD-No ACLF and AD-ACLF, respectively),[31] the recent PREDICT study identified that AD-No ACLF is a heterogenous condition with three distinct clinical courses.[5] We have assigned all patients in the AD-No ACLF group to one of the three clinical trajectories as per the PREDICT study (stable decompensated cirrhosis (SDC), unstable decompensated cirrhosis (UDC) and pre-ACLF). Thirty-two per cent of the patients with AD did not require any hospital readmission within the 3-month follow-up period (SDC). Fifty-two per cent developed UDC without ACLF and either had a high mortality rate at 3 months or required at least one readmission within the 3 months follow-up period. No patients were assigned to the pre-ACLF trajectory (16% of the AD group were not included in any of the trajectories due no recorded deaths and no-readmissions during the first 3-month follow-up period). The expansion of the CD4$^+$HLA-G$^+$ T cells was most significant in the UDC group, the second most severe course of AD. Analyses in the pre-ACLF group corresponding to the most severe course of AD were not feasible due to the limited sample size in this clinical phenotype. No differences in the distribution of CD4$^+$HLA-G$^+$ T cells were observed according to the number or type of PE to AD (online supplemental figure S2).

CD4$^+$HLA-G$^+$ T cells from patients with AD display a CTLA-4^{high}IL-35^{high}IL-10^{low} phenotype

We further defined this population in the AD group with regard to the expression of cell surface inhibitory markers (Tim3, PD1, CD40L and CTLA-4) and found that CTLA-4 was significantly

Gut: first published as 10.1136/gutjnl-2021-324071 on 3 August 2021. Downloaded from http://gut.bmj.com/ on April 17, 2024 by guest. Protected by copyright.

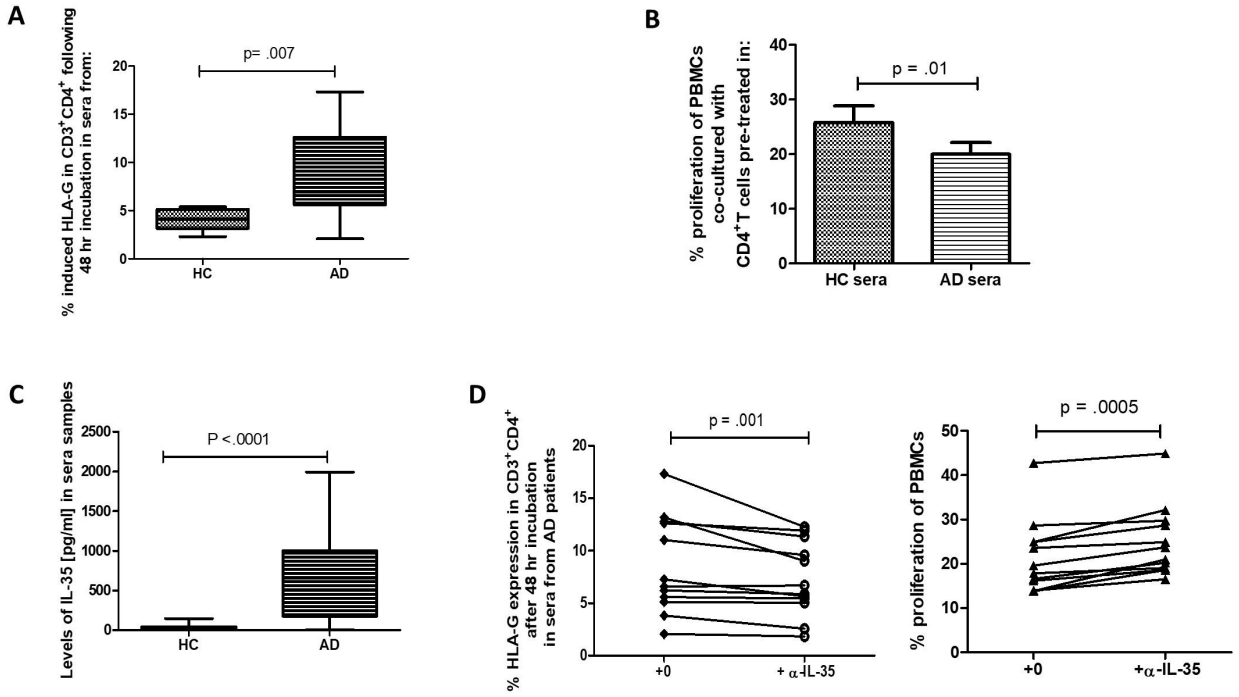

Figure 4 Sera conditioning and the role of interleukin (IL)-35 in inducing CD4$^+$HLA-G$^+$ suppressor cells. (A) Assessment of the effect of sera at inducing HLA-G$^+$ phenotype in cultured CD4$^+$ T cells from healthy controls (HCs) following 48 hours of culture in the presence of 25% sera from HCs and patients with acute decompensation of cirrhosis (AD) (n=15 per group). (B) Proliferation of HC peripheral blood mononuclear cells (PBMCs) in the presence of HC or AD sera-induced human leucocyte antigen G (HLA-G) expression in CD4$^+$ T cells (results are representative of seven independent experiments). (C) Concentrations of IL-35 in sera samples were measured in HCs (n=25) and patients with AD (n=25). (D) Measurement of the role of IL-35 in driving the HLA-G-positive phenotype (left panel) and its effect on proliferation responses (right panel). Anti-IL-35 neutralising antibody (α-IL-35, used at 10 µg/mL) (n=12) was used to block IL-35 prior to sera exposure. This was suppressed when sera from patients with AD were pretreated with neutralising IL-35 antibody. Mann-Whitney U test for two group comparison and Wilcoxon matched pairs signed rank test was used for all paired non-parametric tests. Data are presented as median values with IQR.

co-expressed by CD4$^+$HLA-G$^+$ T cells in patients with AD compared with HCs (figure 2A). This was not observed in the HLA-G-negative fraction (online supplemental figure S3A). No significant changes were detected in the expression of the other tested inhibitory markers (online supplemental figure S3B). When screened for anti-inflammatory/suppressive cytokines (IL-35 and IL-10), CD4$^+$HLA-G$^+$ cell subsets from patients with AD demonstrated increased IL-35 expression compared with HCs (figure 2B). Unlike IL-35, IL-10 was expressed in a significantly lower proportion of the HLA-G$^+$ cells (figure 2C). In addition, we noted that IL-35 was mostly elevated in HLA-G$^+$ cells when compared with CD25^{high}CD127^{low} tTregs (online supplemental figure S3C).

Transcriptional and functional characteristics of CD4$^+$HLA-G$^+$ T cells from patients with AD

Next, we performed gene expression profiling of the CD4$^+$HLA-G$^+$ population and to determine whether it was distinguishable from tTreg population and the HLA-G-negative counterpart. Three distinct populations were cell sorted based on the gating strategy depicted in online supplemental figure S1A. First, CD4$^+$ T cells from four different patients with AD were separated into two main populations: CD25^{high}CD127^{Low} tTregs and CD25$^-$CD127^{high} non-tTregs. HLA-G$^+$ and HLA-G$^-$ T cells were then sorted from the tTreg-depleted population. Differential expression of the analysed genes between the three subsets was revealed (figure 3A).

The HLA-G$^+$ subset displayed a distinct gene expression pattern from tTregs. This was evidenced by significant downregulation of tTreg-specific signature genes *FOXP3 and IL2RA*, regulators of tTreg function genes (*FCRL3*, *EZH2*, *CD27*, *TRAF3* and *TIGIT*) and an upregulation in *IL7R* (*CD127*) gene (figure 3B and online supplemental figure S4A). Genes involved in susceptibility to apoptosis/necrosis (*CASP3*, *RIPK3*, *FAS*) and proliferation, differentiation and IL-2 production (*TRAF1*, *TRIM21*) were also downregulated in HLA-G$^+$ compared with tTregs, while regulators of inflammation such as LTB and SOCS3 were significantly upregulated (figure 3B and online supplemental figure S4A).

Compared with the HLA-G$^-$ subset, HLA-G$^+$ cells exhibited increased expression of genes important for the induction of regulation and suppression (*TNFRSF1B* and *CD52*), epigenetic regulators (*HIST1H4H*, *HIST1H2BK*, *HIST1H2BF*) and markers of activation (*NKG7*, *FCGR3A/B*). Notably, HLA-G$^+$ population showed an upregulation in genes involved in exocytosis of CTLA-4 (*ARF1* and *PLD*), supporting the phenotypic findings of enhanced CTLA-4 surface levels (figure 3B and online supplemental figure S4A).

HLA-G$^+$ cells from patients with AD exhibit suppressive properties

CD4$^+$ T cells expressing HLA-G have been shown to act as suppressive cells by dampening lymphocyte-driven immune responses.[32 33] To explore their regulatory capacity in patients with AD, magnetically cell-sorted CD4$^+$HLA-G$^+$ T cells were incubated at increasing ratios with CPD-labelled allogeneic PBMCs in the presence of anti-CD3 polyclonal stimulation. Here, we show that purified HLA-G$^+$ cells had a strong suppressive

Gut: first published as 10.1136/gutjnl-2021-324071 on 3 August 2021. Downloaded from http://gut.bmj.com/ on April 17, 2024 by guest. Protected by copyright.

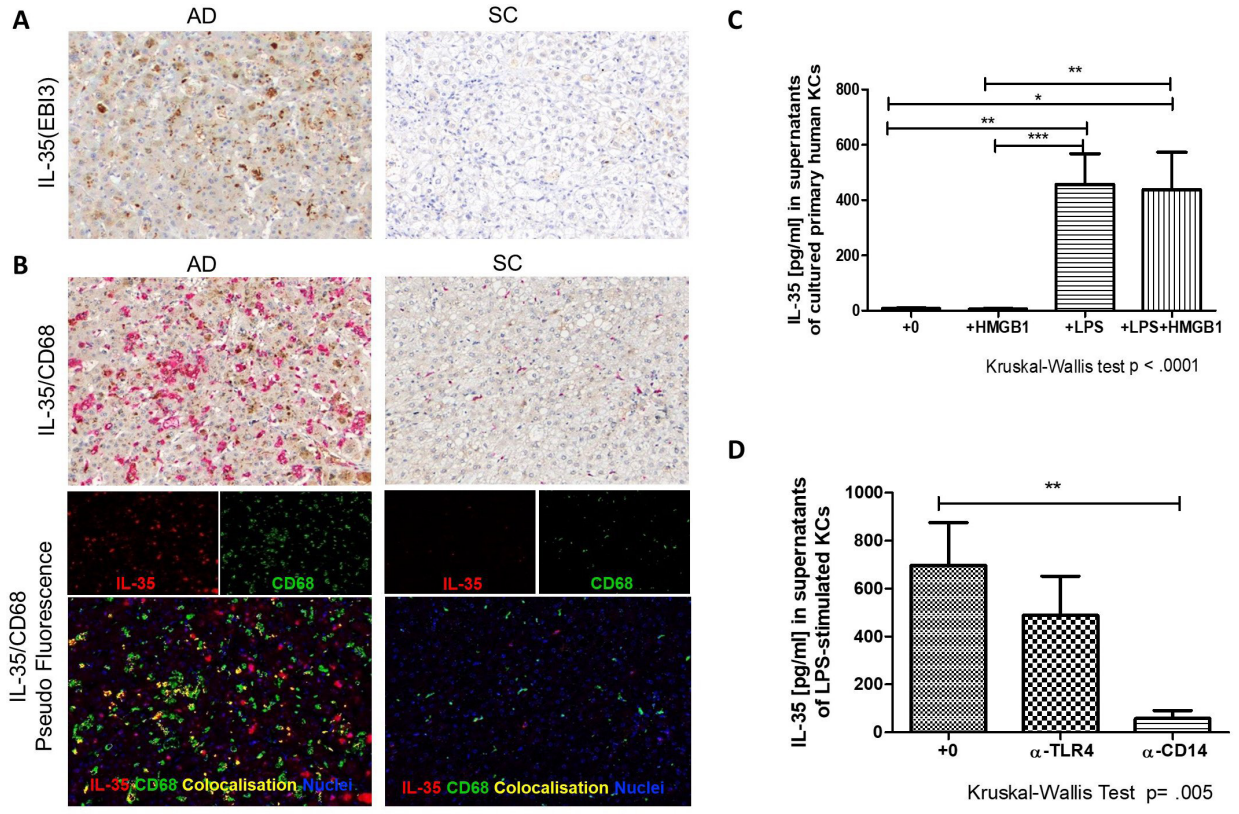

Figure 5 Immunohistochemical and in vitro evaluation of sources of interleukin (IL)-35 from diseased liver. (A) Immunohistochemistry (IHC) was used to detect and quantify IL-35 (EBI3) in liver explants tissues of patients with acute decompensation of cirrhosis (AD) compared with pathological stable cirrhosis (SC) control (alcohol-related cirrhosis). Single stain for IL-35, detected using DAB (brown), nuclei detected using haematoxylin (blue) with 200× magnification. (B) Double stain for IL-35 (brown) and intrahepatic CD68$^+$ tissue Kupffer cells (KCs) (CD68 detected using Permanent Red (red)). Nuclei were detected using haematoxylin (blue) with 200× magnification (top panels). For pseudofluorescence, IL-35, CD68 and nuclei were visualised by red, green and blue, respectively. Co-localisation of IL-35 and CD68 was visualised by yellow (bottom panels). (C) Human primary KCs were assessed for their capacity to secrete IL-35 in vitro following no stimulation (n=9), stimulation with high mobility group box 1 (HMGB1) (n=9) or *Escherichia coli* lipopolysaccharide (LPS) (n=10) and simultaneous stimulation with both LPS +HMGB1 (n=9). ELISA was used to detect IL-35 concentrations in collected supernatants following 48 hours incubation. (D) Receptors involved in the signalling pathways were tested for their role in the LPS-induced IL-35 secretion through blockade of CD14 (n=6) and toll-like receptor 4 (TLR-4) receptors (n=6). Kruskal-Wallis followed by a Dunn's test for multiple comparisons between more than two groups. Data are presented as median values with IQR. *P<0.05; **p<0.005; ***p<0.0005.

activity on proliferating responder CD3$^+$ T cells with a more pronounced percentage of suppression at lower responder-to-HLA-G$^+$ ratio of 16:1 and 8:1 (55% (27.12–74.33) and 69.73% (39.68–85.54), respectively) (figure 3C). Despite the loss of a suppressor ratio-dependent suppressive effect at higher ratios, HLA-G$^+$ cells still retained a strength of suppression above 50% (figure 3C). Furthermore, HLA-G$^+$ cells were up to 2.5-fold more suppressive than the non-HLA-G expressing cell fraction (online supplemental figure S4B,C).

In vitro conditioning in AD-derived sera induces the suppressive CD4$^+$HLA-G$^+$

We have previously reported that soluble mediators in the sera of patients with liver disease can induce phenotypic and functional properties resembling those detected ex vivo in circulating leucocytes from patients.[15 34] As shown in figure 4A, in vitro exposure of healthy CD4$^+$ T cells to sera from patients with AD resulted in enhancement of HLA-G surface expression; no such elevation was observed after exposure to sera from HCs or a pathological control (online supplemental figure S5A). Similar to HLA-G$^+$ cells from patients with AD, in vitro AD sera-induced CD4$^+$HLA-G$^+$ had a suppressive capacity to significantly inhibit PBMCs proliferation as detected by reduction in the percentages of proliferating responder lymphocytes (figure 4B).

Elevated circulating IL-35 in decompensated disease mediates induction of CD4$^+$HLA-G$^+$ suppressor T cells

Having detected high levels of intracellular IL-35 in the HLA-G expressing cells, we measured the levels of this immunosuppressive cytokine in the circulation. Concentrations of IL-35 were mostly elevated in sera from patients with AD compared with HCs (figure 4C). Notably, levels of IL-35 were markedly increased in patients with AD when compared with a pathological control (online supplemental figure S5B).

In addition to its production by several peripherally derived Tregs, IL-35 has also been reported to be involved in their development and expansion.[27 29 35] Thus, we then examined whether elevated IL-35 levels present in sera from patients with AD were capable of inducing the HLA-G$^+$ phenotype. To test this, we neutralised IL-35 in AD sera before exposure to CD4$^+$ T cells and demonstrated that this abolished sera-induced HLA-G upregulation (figure 4D) and yielded cells with a substantially reduced suppressive function as demonstrated by restored proliferation in responder T cells (figure 4D). These changes were not

Gut: first published as 10.1136/gutjnl-2021-324071 on 3 August 2021. Downloaded from http://gut.bmj.com/ on April 17, 2024 by guest. Protected by copyright.

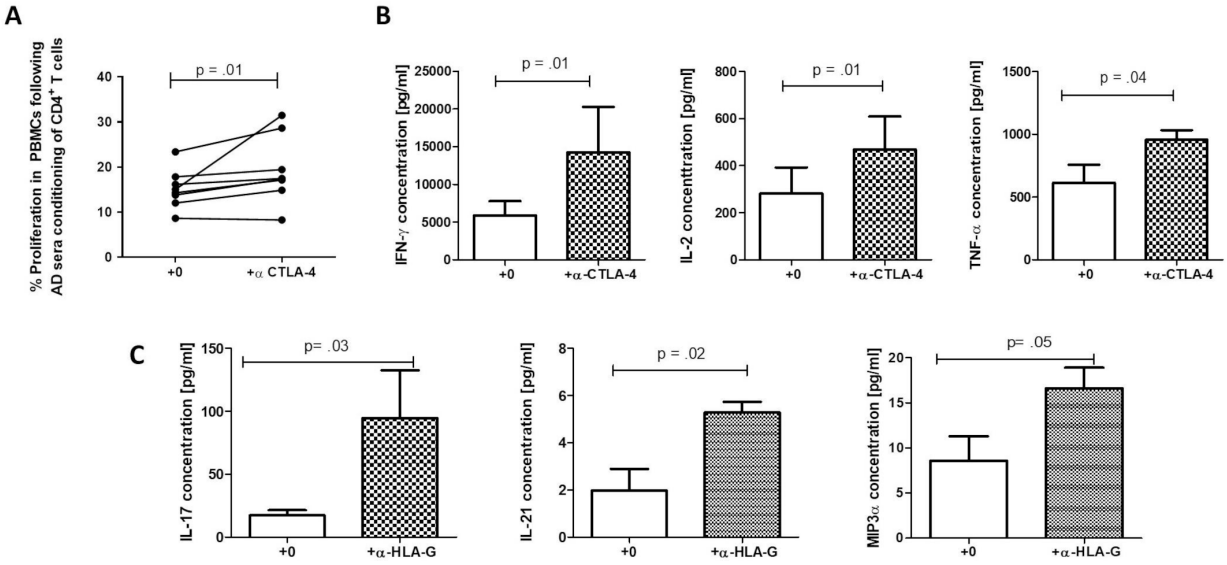

Figure 6 $CD4^+HLA\text{-}G^+$ T cells suppressive capacity is reversed following blockade of cytotoxic T lymphocyte antigen-4 (CTLA-4), whereas blockade of human leucocyte antigen G (HLA-G) impairs T helper 17 (Th17)-related cytokine secretion. (A) HLA-G expressing cells generated following preconditioning of $CD4^+$ T cells in sera from patients with acute decompensation of cirrhosis (AD) were tested for their capacity to suppress proliferating peripheral blood mononuclear cells (PBMCs) in the presence of absence of α-CTLA-4 (10 µg/mL) (n=8). (B) Levels of cytokines playing a role in T cell proliferation/function in supernatants collected following 5-day co-cultures of $CD4^+HLA\text{-}G^+$ T cells with PBMCs with or without α-CTLA-4 were measured using multiplex cytokine detection system (n=8). (C) Blockade of HLA-G restored production of Th17-related cytokines/chemokines. Wilcoxon matched pairs signed rank test was used for all paired non-parametric tests. Data are presented as median values with IQR.

observed with blockade of IL-35 prior to conditioning in sera from HC or SC (online supplemental figure S5C,D). Furthermore, we show that IL-10, another immunosuppressive cytokine, was not relevant in the induction of this phenotype (online supplemental figure S5E).

Cellular sources of IL-35

Elevated levels of IL-35 in sera suggested that other cell populations may contribute to the release of this immunosuppressive cytokine. Using IHC analyses we detected high expression of IL-35 that co-localised with KCs in liver sections from patients with AD (figure 5A and B). Levels were undetectable in SC. To further dissect this finding, we investigated the capacity of isolated human primary KCs to produce IL-35 in vitro and tested the contribution of key triggers of liver injury comprising danger-associated or pathogen-associated molecular patterns (DAMPS or PAMPS) towards this secretion. Only stimulation with a well-known PAMP (LPS), but not a major DAMP (HMGB1) led to a significant increase in IL-35 secretion from cultured KCs (figure 5C). No further increase in the concentration of LPS-induced IL-35 was detected by concurrent treatment with HMGB1 (figure 5C). TLR4 and CD14 are pivotal receptors required for cytokine production from KC in response to LPS signalling.[36] Similar to LPS, HMGB1 capacity to induce cytokine secretion requires signalling through TLR4.[37] In this regard, we sought to confirm the role of the two receptors in the LPS-induced secretion of IL-35 using blocking antibodies and demonstrated that IL-35 induction was abrogated following CD14 blockade (figure 5D).

$CD4^+HLA\text{-}G^+$ cells suppression of responder T cell responses is CTLA-4-mediated

Given the detected upregulation of key negative regulator CTLA-4 as well as genes involved in its membrane recycling and expression, we decided to assess its role in the suppressive mechanism of the $HLA\text{-}G^+$ population. Blockade of CTLA-4 attenuated the capacity of AD-sera-induced, but not HC-sera-induced, $HLA\text{-}G^+$ T cells to suppress responder T cells proliferation (figure 6A and online supplemental figure S6A). Furthermore, it restored key T cell proliferation cytokine secretion, including interferon-γ, tumour necrosis factor-α and IL-2 (figure 6B). Of note, blockade of immunomodulatory factors HLA-G and IL-35 did not abrogate the suppressive capacity of the described population (online supplemental figure S6B). However, neutralisation of HLA-G, but not CTLA-4 or IL-35, specifically restored production of Th17-related cytokines/chemokines including IL-17, IL-21 and macrophage inflammatory protein-3alpha (figure 6C and online supplemental figure S6C).

DISCUSSION

This study identifies an expansion of an IL-35-induced HLA-G-expressing regulatory $CD4^+$ T subpopulation exerting suppressive properties via distinct and specific mechanisms of action, namely (1) a CTLA-4-dependent pathway delineated by the capacity to reduce T cell proliferation and diminish production of cytokines essential for T cell functions and (2) an HLA-G-driven inhibition of cytokines specifically related to Th17 responses. Proportions of the $CD4^+HLA\text{-}G^+$ T cells were associated with disease severity, susceptibility to infections and poor outcome.

HLA-G, a non-classical HLA class I molecule, was originally described as a regulator of tolerance; conferring protection against foetal rejection, tolerance to allografts and contributing to immune escape mechanisms in cancer and viral infections.[38 39] Reports on expression of HLA-G on lymphocytes were first described in patients with HIV.[40] Studies led by Feger *et al* were the first to report HLA-G expression by T cells with regulatory capacity present at low levels in healthy blood.[32] The same group further defined cellular and molecular characteristics of this population and demonstrated its important role in peripheral immune regulation in inflammatory disorders such as multiple

Gut: first published as 10.1136/gutjnl-2021-324071 on 3 August 2021. Downloaded from http://gut.bmj.com/ on April 17, 2024 by guest. Protected by copyright.

sclerosis and in graft-versus-host disease.[41 42] In line with these previously reported suppressive HLA-G$^+$ T cells,[32] cells from patients with AD were clearly distinguished from tTregs by their immunological gene signature demonstrating a lack of *FOXP3* and *IL2RA* (coding gene for CD25) and marked upregulation of *IL7R* (gene encoding for CD127).

In previous studies, CD4$^+$HLA-G$^+$ cells from healthy individuals were reported to produce high levels of IL-10 and exert their suppression in an IL-10-dependent manner.[33] In contrast, CD4$^+$HLA-G$^+$ T cells from patients with AD were weak producers of IL-10 suggesting that their suppressive functions were unlikely to be supported by IL-10. Here, using in vitro suppression assays, we demonstrated that the inhibition of alloreactive T cell proliferation by HLA-G$^+$ subset was mediated through CTLA-4 signalling. We have previously identified and characterised negative regulation of adaptive immune responses mediated by CTLA-4-expressing CD4$^+$ T cells in the settings of acute liver failure (ALF).[34] Taken together, our studies suggest a major immunomodulatory role of CTLA-4 in ALF and chronic liver failure and that blockade of this pathway may be beneficial in restoring T cell-mediated responses. Growing clinical experience of the risks of immune-mediated adverse reactions using established targeted anti-CTLA therapies (eg, checkpoint inhibitor (CPI)-induced liver injury) has given pause to this strategy of immune modulation,[43] and would require significant caution in end-stage liver disease. Modulation of immune cell metabolism has been considered as an adjunct to immune CPI in patients with cancer.[44] This suggests the need for further studies to explore whether the loss of HLA-G$^+$ T cells' inhibitory capacity through CTLA-4 blockade is accompanied by changes in cellular metabolites to determine possible metabolic targets in decompensated cirrhosis. In tumour-bearing mouse models, HLA-G was shown to promote immune evasion through expansion of myeloid-derived suppressor cells and alteration of cytokine balance through inhibition of Th1/Th17 responses.[45] Indeed, our findings support an important role for HLA-G in suppressing Th17 responses; a crucial immune response in host defence against a variety of pathogens, including bacteria and viruses.[46] Further investigations are needed to dissect how myeloid lineages, particularly antigen-presenting cells exhibiting elevated levels of ILT4 (HLA-G receptor), may account for the impairment in promoting Th17 differentiation.

This work has established a role of the anti-inflammatory cytokine IL-35 in inducing the HLA-G$^+$ phenotype in patients with AD. Although secreted by the HLA-G$^+$ cells, higher levels of IL-35 seemed to originate in KCs following challenge from LPS. We therefore postulate that continuous exposure to gut-derived bacterial products through increased bacterial translocation in AD[47] is likely to explain the induction and release of IL-35 from specialised cells in the inflamed liver which can reach the circulation. Consistent with our observations, Collison *et al* demonstrated that IL-35 promoted Tregs induction and maintenance and that IL-35-treated cells were also capable to secrete IL-35[35]. Interestingly, a population of IL-35-induced CD4$^+$ Tregs, named iT$_r$35 did not express IL-10 and were suppressive of responder T cells proliferation primarily through an IL-35-dependent manner. In our study however, in vitro blockade of IL-35 failed to disable the suppressive function of CD4$^+$HLA-G$^+$ cells, suggesting that IL-35 might not be required for their suppressive capacity but for the generation and possibly the maintenance of this population. However, further studies are required to investigate possible roles of IL-35 in initiating the suppressive cascade and in contributing to the maximal HLA-G$^+$ T cell suppressive function. Evidence also suggests a role for IL-35 in generating IL-35-secreting regulatory B cells, which can then induce Tregs.[48] It is therefore pertinent to further investigate the effect of the IL-35-secreting-HLA-G$^+$ subpopulation on modulating other adaptive cell functions, such as B cells.

Clinically, when examined for correlation with infectious complications, the studied T cell subset was elevated in patients who developed culture positive and short-term infections. Additionally, it correlated with indicators of infection and inflammation, such as CRP and WCC. HLA-G-expressing CD4$^+$ T cells could therefore be used as a useful marker alongside currently used surrogate indicators of disease severity and adverse outcome in patients with AD and might have potential prognostic implications. Therapeutic effectiveness of HLA-G blockade using TTX-080, a monoclonal antibody targeting HLA-G, is currently underway in clinical trials of patients with solid tumours.[49] In addition, combination therapy targeting HLA-G concomitantly with other immune CPIs has been suggested in non-responder patients with cancer to CPI monotherapy.[50] However, early results from the current clinical trials are required before further consideration of this treatment strategy. Additionally, the frequency of circulating CD4$^+$HLA-G$^+$ T cells could be used as a potential predictor of the three newly identified clinical courses of AD.[5] However, these findings require further investigations in larger patient populations with the view to better understand all three clinical courses of AD.

In addition to quantitative impairment in circulating T cells reported in AD, including AD-ACLF,[51] our findings indicate that elevated proportions of the remaining T cells are typified by increased inhibitory receptor expression. Understanding the combination of the quantitative and qualitative impairments in the T cell compartment and its contribution to immuneparesis in chronic liver failure is of crucial importance in providing insights into potential therapeutic targets. Here, we report a potential mechanism of dysregulation in immune responsiveness in patients with AD governed by a CD4$^+$HLA-G$^+$CTLA-4$^+$IL-35$^+$suppressive population associated with possible risk to infections through defects in the systemic adaptive immune system.

Twitter Wafa Khamri @KhamriWafa and Rooshi Nathwani @RooshiNathwani

Acknowledgements The authors would like to thank Professor Robert Goldin (Imperial College London, UK) for methodological support, Dr Amy Anderson (Newcastle University, UK) and Dr Nikhil Vergis (Imperial College London, UK) for useful discussions and all the patients who participated in the study. We thank the NanoString facility at University College London, UK and the St Mary's Flow Cytometry Core Facility at Imperial College London, UK.

Contributors WK initiated and coordinated the study. WK, CJW, CGA and MRT contributed to the conceptualisation and approach to the study. WK, CG, TL, RN, MK, SA, FMT, LP, ET, TB, RCS, FL, AS, SM, MMP, CJW, CGA and MRT contributed to data curation, analyses, investigation, methodology and interpretation of data. RN, FMT, LP, ET, TB, RCS, FL, AS, NK, CB, SM, MMP and CJW provided and contributed to supporting methodology, supporting resources and material. WK, CG, TL, RN and SM wrote the original draft. WK, TL, RN, FMT, LP, ET, FL, AS, CB, SM, MMP, CW and MRT contributed to the reviewing and editing of the original draft. WK, CJW, CA and MT acquired funding.

Funding This study was supported by the NIHR Imperial Biomedical Research Centre (BRC), Institute for Translational Medicine and Therapeutics (ITMAT) (74713), Medical Research Council (MRC) (MR/K010514/1 and MR/R014019/1).

Competing interests None declared.

Patient consent for publication Not required.

Ethics approval This study was approved by the local research ethic committee (LREC (12/LO/0167)) and was performed in accordance with the Declaration of Helsinki.

Provenance and peer review Not commissioned; externally peer reviewed.

Data availability statement All data relevant to the study are included in the article or uploaded as supplementary information.

Author note CGA and MRT are joint last authors.

Gut: first published as 10.1136/gutjnl-2021-324071 on 3 August 2021. Downloaded from http://gut.bmj.com/ on April 17, 2024 by guest. Protected by copyright.

Supplemental material This content has been supplied by the author(s). It has not been vetted by BMJ Publishing Group Limited (BMJ) and may not have been peer-reviewed. Any opinions or recommendations discussed are solely those of the author(s) and are not endorsed by BMJ. BMJ disclaims all liability and responsibility arising from any reliance placed on the content. Where the content includes any translated material, BMJ does not warrant the accuracy and reliability of the translations (including but not limited to local regulations, clinical guidelines, terminology, drug names and drug dosages), and is not responsible for any error and/or omissions arising from translation and adaptation or otherwise.

Open access This is an open access article distributed in accordance with the Creative Commons Attribution 4.0 Unported (CC BY 4.0) license, which permits others to copy, redistribute, remix, transform and build upon this work for any purpose, provided the original work is properly cited, a link to the licence is given, and indication of whether changes were made. See: https://creativecommons.org/licenses/by/4.0/.

ORCID iDs
Wafa Khamri http://orcid.org/0000-0001-9101-8457
Rooshi Nathwani http://orcid.org/0000-0002-5069-7956
Evangelos Triantafyllou http://orcid.org/0000-0002-2755-9619
Mark McPhail http://orcid.org/0000-0001-5449-2424

REFERENCES

1 Martínez-Esparza M, Tristán-Manzano M, Ruiz-Alcaraz AJ, *et al*. Inflammatory status in human hepatic cirrhosis. *World J Gastroenterol* 2015;21:11522–41.
2 Bataller R, Brenner DA. Liver fibrosis. *J Clin Invest* 2005;115:209–18.
3 Arroyo V, Moreau R, Jalan R. Acute-on-chronic liver failure. *N Engl J Med* 2020;382:2137–45.
4 Trebicka J, Fernandez J, Papp M, *et al*. PREDICT identifies precipitating events associated with the clinical course of acutely decompensated cirrhosis. *J Hepatol* 2021;74:33772–7.
5 Trebicka J, Fernandez J, Papp M, *et al*. The PREDICT study uncovers three clinical courses of acutely decompensated cirrhosis that have distinct pathophysiology. *J Hepatol* 2020;73:842–54.
6 Wong F, Bernardi M, Balk R, *et al*. Sepsis in cirrhosis: report on the 7th meeting of the International Ascites Club. *Gut* 2005;54:718–25.
7 Bruns T, Zimmermann HW, Stallmach A. Risk factors and outcome of bacterial infections in cirrhosis. *World J Gastroenterol* 2014;20:2542–54.
8 Albillos A, Lario M, Álvarez-Mon M. Cirrhosis-associated immune dysfunction: distinctive features and clinical relevance. *J Hepatol* 2014;61:1385–96.
9 Malik R, Mookerjee RP, Jalan R. Infection and inflammation in liver failure: two sides of the same coin. *J Hepatol* 2009;51:426–9.
10 Berry PA, Antoniades CG, Carey I, *et al*. Severity of the compensatory anti-inflammatory response determined by monocyte HLA-DR expression may assist outcome prediction in cirrhosis. *Intensive Care Med* 2011;37:453–60.
11 Bernsmeier C, Pop OT, Singanayagam A, *et al*. Patients with acute-on-chronic liver failure have increased numbers of regulatory immune cells expressing the receptor tyrosine kinase MERTK. *Gastroenterology* 2015;148:603–15.
12 Bernsmeier C, Triantafyllou E, Brenig R, *et al*. $CD14^+$ $CD15^-$ HLA^-DR^- myeloid-derived suppressor cells impair antimicrobial responses in patients with acute-on-chronic liver failure. *Gut* 2018;67:1155–67.
13 Bernsmeier C, van der Merwe S, Périanin A. Innate immune cells in cirrhosis. *J Hepatol* 2020;73:186–201.
14 Brenig R, Pop OT, Triantafyllou E, *et al*. Expression of AXL receptor tyrosine kinase relates to monocyte dysfunction and severity of cirrhosis. *Life Sci Alliance* 2020;3:e201900465.
15 Lebossé F, Gudd C, Tunc E, *et al*. Cd8+ T cells from patients with cirrhosis display a phenotype that may contribute to cirrhosis-associated immune dysfunction. *EBioMedicine* 2019;49:258–68.
16 Buckner JH, Ziegler SF. Regulating the immune system: the induction of regulatory T cells in the periphery. *Arthritis Res Ther* 2004;6:215–22.
17 Lan R, Ansari A, Lian Z, *et al*. Regulatory T cells: development, function and role in autoimmunity. *Autoimmun Rev* 2005;4:351–63.
18 Han Y, Guo Q, Zhang M, *et al*. Cd69+ CD4+ CD25- T cells, a new subset of regulatory T cells, suppress T cell proliferation through membrane-bound TGF-beta 1. *J Immunol* 2009;182:111–20.
19 Abbas AK, Benoist C, Bluestone JA, *et al*. Regulatory T cells: recommendations to simplify the nomenclature. *Nat Immunol* 2013;14:307–8.
20 Kovats S, Main E, Librach C, *et al*. A class I antigen, HLA-G, expressed in human trophoblasts. *Science* 1990;248:220–3.
21 Creput C, Le Friec G, Bahri R, *et al*. Detection of HLA-G in serum and graft biopsy associated with fewer acute rejections following combined liver–kidney transplantation: possible implications for monitoring patients. *Hum Immunol* 2003;64:1033–8.
22 Carosella ED, Favier B, Rouas-Freiss N, *et al*. Beyond the increasing complexity of the immunomodulatory HLA-G molecule. *Blood* 2008;111:4862–70.
23 Naji A, Le Rond S, Durrbach A, *et al*. CD3+CD4low and CD3+CD8low are induced by HLA-G: novel human peripheral blood suppressor T-cell subsets involved in transplant acceptance. *Blood* 2007;110:3936–48.
24 Pankratz S, Ruck T, Meuth SG, *et al*. CD4+HLA-G+ regulatory T cells: molecular signature and pathophysiological relevance. *Hum Immunol* 2016;77:727–33.
25 Lemaoult J, Zafaranloo K, Le Danff C, *et al*. HLA-G up-regulates ILT2, ILT3, ILT4, and KIR2DL4 in antigen presenting cells, NK cells, and T cells. *FASEB j.* 2005;19:1–23.
26 LeMaoult J, Krawice-Radanne I, Dausset J, *et al*. HLA-G1-expressing antigen-presenting cells induce immunosuppressive CD4+ T cells. *Proc Natl Acad Sci U S A* 2004;101:7064–9.
27 Niedbala W, Wei X-Q, Cai B, *et al*. Il-35 is a novel cytokine with therapeutic effects against collagen-induced arthritis through the expansion of regulatory T cells and suppression of Th17 cells. *Eur J Immunol* 2007;37:3021–9.
28 Vignali DAA, Kuchroo VK. Il-12 family cytokines: immunological playmakers. *Nat Immunol* 2012;13:722–8.
29 Collison LW, Workman CJ, Kuo TT, *et al*. The inhibitory cytokine IL-35 contributes to regulatory T-cell function. *Nature* 2007;450:566–9.
30 McMurchy AN, Levings MK. Suppression assays with human T regulatory cells: a technical guide. *Eur J Immunol* 2012;42:27–34.
31 Moreau R, Jalan R, Gines P. Acute-On-Chronic liver failure is a distinct syndrome that develops in patients with acute decompensation of cirrhosis. *Gastroenterology* 2013;144:1426–37.
32 Feger U, Tolosa E, Huang Y-H, *et al*. HLA-G expression defines a novel regulatory T-cell subset present in human peripheral blood and sites of inflammation. *Blood* 2007;110:568–77.
33 Huang Y-H, Zozulya AL, Weidenfeller C, *et al*. T cell suppression by naturally occurring HLA-G-expressing regulatory CD4+ T cells is IL-10-dependent and reversible. *J Leukoc Biol* 2009;86:273–81.
34 Khamri W, Abeles RD, Hou TZ, *et al*. Increased expression of cytotoxic T-Lymphocyte-Associated protein 4 by T cells, induced by B7 in sera, reduces adaptive immunity in patients with acute liver failure. *Gastroenterology* 2017;153:263–76.
35 Collison LW, Chaturvedi V, Henderson AL, *et al*. IL-35-mediated induction of a potent regulatory T cell population. *Nat Immunol* 2010;11:1093–101.
36 Lee CC, Avalos AM, Ploegh HL. Accessory molecules for Toll-like receptors and their function. *Nat Rev Immunol* 2012;12:168–79.
37 Yang H, Wang H, Ju Z, *et al*. MD-2 is required for disulfide HMGB1-dependent TLR4 signaling. *J Exp Med* 2015;212:5–14.
38 Le Bouteiller P, Blaschitz A. The functionality of HLA-G is emerging. *Immunol Rev* 1999;167:233–44.
39 Bainbridge DR, Ellis SA, Sargent IL. HLA-G suppresses proliferation of CD4(+) T-lymphocytes. *J Reprod Immunol* 2000;48:17–26.
40 Lozano JM, González R, Kindelán JM, *et al*. Monocytes and T lymphocytes in HIV-1-positive patients express HLA-G molecule. *AIDS* 2002;16:347–51.
41 Huang Y-H, Zozulya AL, Weidenfeller C, *et al*. Specific central nervous system recruitment of HLA-G(+) regulatory T cells in multiple sclerosis. *Ann Neurol* 2009;66:171–83.
42 Pankratz S, Bittner S, Herrmann AM, *et al*. Human CD4+ HLA-G+ regulatory T cells are potent suppressors of graft-versus-host disease in vivo. *Faseb J* 2014;28:3435–45.
43 Grosso JF, Jure-Kunkel MN. CTLA-4 blockade in tumor models: an overview of preclinical and translational research. *Cancer Immun* 2013;13:5.
44 Melero I, Berman DM, Aznar MA, *et al*. Evolving synergistic combinations of targeted immunotherapies to combat cancer. *Nat Rev Cancer* 2015;15:457–72.
45 Agaugué S, Carosella ED, Rouas-Freiss N. Role of HLA-G in tumor escape through expansion of myeloid-derived suppressor cells and cytokinic balance in favor of Th2 versus Th1/Th17. *Blood* 2011;117:7021–31.
46 Tesmer LA, Lundy SK, Sarkar S, *et al*. Th17 cells in human disease. *Immunol Rev* 2008;223:87–113.
47 Wiest R, Lawson M, Geuking M. Pathological bacterial translocation in liver cirrhosis. *J Hepatol* 2014;60:197–209.
48 Wang R-X, Yu C-R, Dambuza IM, *et al*. Interleukin-35 induces regulatory B cells that suppress autoimmune disease. *Nat Med* 2014;20:633–41.
49 Liu L, Wang L, Zhao L, *et al*. The role of HLA-G in tumor escape: manipulating the phenotype and function of immune cells. *Front Oncol* 2020;10:597468.
50 Dumont C, Jacquier A, Verine J, *et al*. $CD8^+PD\text{-}1^+ILT2^+$ T Cells Are an Intratumoral Cytotoxic Population Selectively Inhibited by the Immune-Checkpoint HLA^-G. *Cancer Immunol Res* 2019;7:1619–32.
51 Weiss E, de la Grange P, Defaye M, *et al*. Characterization of blood immune cells in patients with decompensated cirrhosis including ACLF. *Front Immunol* 2020;11:619039.

Gut: first published as 10.1136/gutjnl-2021-324071 on 3 August 2021. Downloaded from http://gut.bmj.com/ on April 17, 2024 by guest. Protected by copyright.

Supplementary Materials for

Suppressor CD4$^+$ T cells expressing HLA-G are expanded in the peripheral blood from patients with acute decompensation of cirrhosis

Wafa Khamri[1*], Cathrin L. Gudd[1], Tong Liu[1], Rooshi Nathwani[1], Marigona Krasniqi[1], Sofia Azam[1], Thomas Barbera[1], Francesca M. Trovato[2], Lucia A. Possamai[1], Evangelos Triantafyllou[1], Rocio Castro Seoane[1], Fanny Lebosse[1], Arjuna Singanayagam[1], Naveenta Kumar[1], Christine Bernsmeier[1,2], Sujit Mukherjee[1], Mark J.W. McPhail[2], Christopher J. Weston[3], Charalambos G. Antoniades[1¶] and Mark R. Thursz [1¶]

¶ Authors share last co-authorship

*** Corresponding author:**

Dr Wafa Khamri

Imperial College, Liver Immunology Laboratory

Division of Digestive Disease

Department of Metabolism, Digestion & Reproduction

10th Floor QEQM Wing, St Mary's Campus

South Warf Road

W2 1NY London, UK

Tel: +44 (0) 203 3126454

Email: w.khamri@imperial.ac.uk

Supplementary information Content:

- **Supplementary Material and Methods**
- **Supplementary Figures and Figure legends (S1-S6)**
- **Supplementary Table (Table S1)**

Khamri W, *et al. Gut* 2021;0:1–11. doi: 10.1136/gutjnl-2021-324071

Patients characteristics

Informed consent was obtained from patients or if the patient lacked capacity, assent was sought from the next of kin. All patients with a diagnosis of cirrhosis, made either clinically and/or biochemically and/or radiologically and/or histologically, admitted to hospital were screened for study suitability within 72 hours of admission. Exclusion criteria were the following: patients younger than 18 years; current viral infection (Hepatitis A, B, C and E virus or Human Immunodeficiency Virus); malignancy; *Clostridium difficile* infection; immunosuppression (excluding low dose steroids or steroid sparing agents for autoimmune hepatitis treatment - < 20mg or equivalent of prednisolone), estimated glomerular filtration rate (eGFR) < 30 on screening ± randomisation, end-stage/severe cardiac, pulmonary or kidney disease, Type 1 Diabetes Mellitus, colitis or coeliac disease and pregnancy. Inclusion criteria were clinical ± biochemical ± radiology ± histological diagnosis of cirrhosis, hospital admission with complication of cirrhosis including alcoholic hepatitis, sepsis, variceal haemorrhage, ascites, renal dysfunction and commencement of antimicrobial therapy.

Primary infections on admission, and second infections defined as infective episode following an initial infection, were defined by published criteria from the North American Consortium for the Study of End-Stage Liver Disease (NACSELD)[45,46].

Peripheral blood mononuclear cell (PBMC) isolation and flow cytometry

PBMCs were isolated from 50 ml of heparin-anticoagulated whole blood through Ficoll-paque™ Plus (GE Healthcare Bio-Sciences AB, Sweden) density-gradient centrifugation, cryopreserved and stored at -80°C. Following fixable viability dye (FVD) staining (Thermo Fisher Scientific, Waltham, MA, USA), PBMCs were surface stained using fluorochrome-labelled mouse anti-human monoclonal antibodies (Supplementary Table S1). For the detection of intracellular levels of IL-35 and IL-10, PBMCs were stained extracellularly for CD3, CD8, CD4 and HLA-G, fixed and then permeabilized according to the manufacturer's instructions using the eBioscience™ Intracellular Fixation & Permeabilization Buffer Set (Thermo Fisher Scientific, USA). Subsequently, intracellular cytokine staining (ICCS) for IL-35 and IL-10 expression was performed. The same staining was also performed on tTregs using CD4, CD25 and CD127 surface staining to detect $CD4^{+}CD25^{+}CD127^{low}$ tTregs (gating strategy in Supplementary Figure 2B). Fluorescence minus one (FMO) were used as controls as depicted in Supplementary Figure 1B. Acquisition of data was performed on the LSR Fortessa™ flow cytometer using BD FACSDiva™ software (Becton Dickinson Ltd, Oxford, UK)

Khamri W, *et al. Gut* 2021;0:1–11. doi: 10.1136/gutjnl-2021-324071

and analyses were performed using FlowLogic software (Inivai Technologies, Pty Ltd).

Quantification of HLA-G expression by real-time PCR

Qiagen RNeasy mini kit (Qiagen, Manchester, UK) was used to extract RNA from magnetic bead-isolated $CD4^+$ T cells (depleted of CD8a, CD14, CD15, CD16, CD19, CD36, CD56, CD123, TcRγ/δ, and CD235a positive cells) (purity was greater than 96%, with less than 1% $CD14^+$ contaminant). This was followed by cDNA synthesis with Bio-rad iScript cDNA synthesis kit (Bio-Rad, Hertfordshire, United Kingdom), according to the manufacturers' instructions. The real-time expression of *HLA-G* was measured by TaqMan gene expression assay using *HLA-G* probe (assay identification number Hs00365950_g1) and compared to paired CD4-negative fractions. Human *GAPDH* (assay identification number Hs02786624_g1) was used as the endogenous control. Quantitative amplification was carried out according to the manufacturer's instructions by using a Step One Plus Real-Time PCR System (Thermo Fisher). Gene expression levels were normalized to *GAPDH* and expressed as fold-change (ratio of $2^{-\Delta\Delta CT}$, $\Delta\Delta CT = \Delta CT_{\text{Patient CD4}^{+/-}\text{ T Cell}} - \Delta CT_{\text{Healthy CD4}^{+}\text{ T Cell}}$).

NanoString gene expression profiling

Prior to Nanostring analyses, PBMCs were subjected to flow-based cell sorting. Surface staining was carried out as described using FVD, CD3, CD4, CD8, HLA-G, CD25 and CD127 (antibodies listed in Supplementary Table S1 and gating strategy in Supplementary Figure S1A). PBMCs from patients with AD (AD-ACLF; n=4) were stained and sorted. First, $CD25^+CD127^{low}$ tTregs were isolated. Then, HLA-G^+ and HLA-G^- populations were sorted from the $CD25^{low}CD127^{high}$ fraction. The sorted cells were lysed using RLT lysis buffer (Qiagen, Germany) and were stored at -80°C. The NanoString assay was performed at the UCL NanoString Facility (University College London, UK). Analyses of 770 immune-related genes were performed in HLA-G^+ T cells and compared to transcriptional profile from purified tTregs and HLA-G^- T cells. Gene expression was reported as log2 fold change of detected mRNA expression levels, normalised to baseline values of tTregs or HLA-G^- T cells. Statistical significance was considered for $p < .05$ and a log2 fold change of 50% higher or lower. Obtained read-count data including quality controls, differential gene expression and volcano plot generation were analysed using the NanoString nSolver™ Analysis Software 4.0 with NanoString Advanced Analysis Module 2.0 plugin (NanoString MAN-C0011-04), following the

NanoString Gene Expression Data Analysis Guidelines (MAN-C0011-04, 2017, MAN-10030-03, 2018).

Immunohistochemistry (IHC)

Liver explants were obtained from liver transplantation of AD patient with AD-ACLF and patient with SC. Single and double heat-induced epitope retrieval immunohistochemistry (IHC) on formalin-fixed paraffin embedded (FFPE) liver tissue was performed to assess the expression of IL-35 (Epstein-Barr virus induced gene 3; EBI3) [(Novus Biologicals, USA) at 1:200 dilution, 12 hours incubation at 4°C] and CD68 [(Dako, Agilent Technologies, USA), ready-to-use, 1 hour incubation at room temperature]. Signal was detected using the EnVision™ G|2 doublestain system – rabbit/mouse (DAB+/permanent red) (Agilent Technologies, Cheshire, UK) detection kit according to the manufacturer's instructions. Images were captured with Nikon Eclipse E600 microscope and double epitope pseudo-fluorescent IHC was used to demonstrate co-localisation by Nuance 3.0.2 multispectral imaging technology (PerkinElmer, Beaconsfield, UK).

Primary human Kupffer cell (KCs) cultures

Cryopreserved primary human Kupffer cells (KCs) (Thermo Fisher Scientific, Hemel Hempstead, UK) were plated on Corning CellBIND 24-well plate (Corning Inc, Tewksbury, USA) at a density of 5×10^5 cells in DMEM medium (Gibco, Hamel Hempstead, UK) with Primary Hepatocyte Maintenance Supplements (Gibco) and cultured at 37°C in 5% CO_2 following manufactures instructions. KCs were then stimulated for 48 hours in the presence of 100 ng/mL *Escherichia coli (E. coli*) lipopolysaccharide (LPS) (Sigma-Aldrich, Dorset, UK) or 100 ng/mL human High-mobility-group-box 1 (HMGB1) (R&D Systems, Abingdon, UK). Prior to LPS or HMGB1 stimulation, KCs were treated with or without 10 µg/ml of anti-Toll-Like Receptor 4 (α-TLR4) (Invivogen, Toulouse, France) or α-CD14 (R&D Systems, Abingdon, UK) blocking antibodies for 45 minutes. Cell culture supernatants were collected for assessment of IL-35 concentrations using ELISA.

Meso scale discovery (MSD) multiplex cytokine detection system

MSD assay was carried out according to the V-PLEX proinflammatory panel 1 (human) protocol for the following cytokines: IFN-γ, IL-1β, IL-2, IL-4, IL-6, IL-10, IL-12p70, IL-13 and TNF-α and the Th17 Panel 1 kit for the following cytokines: IL-17, IL-21, IL-22, IL-23, IL-27, IL-31 and MIP3-α (Meso Scale Discovery System (MSD), Rockville, USA). The assays were carried

out according to the manufacturer's instructions. Prior to the assay, the calibrator dilutions were prepared, and the cytokines were assessed in the cell culture supernatants. The plate was washed three times with 150 μl/well wash buffer (1X PBS and 0.05% Tween-20 (Sigma)), followed by 50 μl/well of standards or samples. The plate was then sealed and incubated for 2 hours with shaking using the Luckham model R100 (Luckham Ltd, Sussex, UK) at room temperature. Subsequently, the plate was washed again and 25 μl of the detection antibody solution added. The plate was sealed again and incubated as before. The plate wash steps were repeated and 150 μl/well of 2X read buffer T was added. The plate was acquired in the SECTOR® S 600 imager using the MSD discovery workbench software (Meso Scale Discovery).

Supplementary Table S1. Markers used for the phenotyping of T cells and monocytes

Laser-Bandpass filter	Flow panels for markers of:	
	T cells	**Monocytes**
Violet 405-450/50	CD3-eFuor 450 [1]	CD1a-eFuor 450 [1]
Violet 405-525/50	CD4-Brilliant Violet 510 [2]	-
Violet 405-780/60	PD-1-Brilliant Violet 786 [2]	-
Violet 405-660/20	-	CD86-Brilliant Violet 650 [1]
Blue 488-530/30	HLA-G-FITC [1]	-
Blue 488-575/26	CTLA-4-PE [1]/ IL-35-PE [3]	CD11c-PE [3]
Blue 488-610/20	Tim3-PE-CF594 [2]/ CD25-PE-CF594 [2]	-
Blue 488-780/60	CD127-PE-Cy7 [1]	CD14-PE-Cy7 [2]
Red 640-670/14	CD8 –APC [1]/ CD40L-APC [1] / IL-10-eFluor 660 [1]	HLA-G-APC [1]/ IL-T4-APC [1]
Red 640-780/60	Fixable Viability Dye (FVD)-eFluor 780 [1]	

[1] *Thermo Fisher Scientific, Hemel Hempstead, UK*

[2] *Becton Dickinson Ltd, Oxford, UK*

[3] *BioLegend, London, UK*

Supplementary Figure S1. Gating strategy used to identify or isolate HLA-G$^+$ cell populations in/from PBMCs. (A) Gating strategy for flow-based cell sorting in preparation for Nanostring analyses. (B) Representative dot plots to define T cell populations expressing HLA-G (Top panel). Lymphocytes were first gated according to the forward and side scatter profile. Doublets were excluded from the analyses using forward scatter height (FSC-H) versus area (FSC-A) discrimination. Dead cells, which were determined by positive staining for the cell viability dye, were then excluded. CD3 then CD4 and CD8 markers were used to determine the lymphocyte primary populations. Monocytes were gated using HLA-DR and CD14 (middle and bottom panels). The double positive population was then gated using CD1a, CD11c and CD86 according to the corresponding FMO controls. (C) Representative histograms of HLA-G expression in CD8$^+$ T cells (left panel) and in monocytes (right panel) from HCs and patients with SC and AD. (D) CD4$^+$ T cells were isolated from PBMCs of HC (n=3) (left panel) and AD patients (AD No-ACLF; n=3, AD-ACLF; n=3) (right panel) and expression of HLA-G mRNA was measured by real-time PCR. Data expressed as fold-change (ratio of $2^{-\Delta\Delta CT}$). (E) Correlation coefficients (r) and correlation p values were tested using non-parametric correlations Spearman test to explore the relationship between the age of the subjects (n=118) and the frequency of CD4$^+$HLA-G$^+$ T cells. Wilcoxon-matched-pairs signed rank test was used for all paired non-parametric tests. Non-parametric (Mann-Whitney) statistical analysis was used. Data are presented as median values with IQR. SSC: side scatter, FSC: forward scatter.

Supplementary Figure S2: Distribution of HLA-G$^+$ T cells in patients with AD according to the number and the type of precipitating events (PE). (A) Distribution of HLA-G$^+$ T cells according to the number of PE (1 PE, and ≥2 PE) to all AD patients, AD-No ACLF and AD-ACLF (left, middle and right panel, respectively). (B) Proportions of HLA-G$^+$ T cells in all patients with AD based on the type of PE (infection vs GI bleed vs active alcohol consumption) alone (top panel) or in combination (bottom panel). (C) Proportions of HLA-G$^+$ T cells in AD-No ALCF based on the type of PE alone (top panel) or in combination (bottom panel). (D) Proportions of HLA-G$^+$ T cells in patients with AD-ALCF based on the type of PE alone (top panel) or in combination (bottom panel).

Supplementary Figure S3. Further phenotypic assessment of HLA-G$^+$ cells in patients with AD. (A) CTLA-4 in HLA-G positive vs negative CD4$^+$ T cells from patients with AD. Representative flow cytometry dot plots/histograms of CTLA-4 expressing cells in CD4$^+$HLA-G$^+$ vs CD4$^+$HLA-G$^-$

T cells (left panel). Proportion of the $CD4^+HLA\text{-}G^+$ vs $CD4^+HLA\text{-}G^-$ T cells expressing CTLA-4 in patients with AD (right panel). (B) Representative histograms of inhibitory markers (Tim3, PD-1 and CD40L) in HLA-G expressing $CD4^+$ T cells (top panel). Levels detected in patients with AD (n=17) compared to HCs (n=10) (bottom panels). (C) Representative dot plots of gating strategy to identify $CD4^+CD25^+CD127^{low}$ tTregs using corresponding FMO controls (left panel). Levels of IL-35 detected using ICCS in $HLA\text{-}G^+$ compared to tTregs from patients with AD (n=11). Non-parametric (Mann-Whitney) statistical analysis was used. Data are presented as median values with IQR.

Supplementary Figure S4. Quantitative microarray gene expression analysis of FACS-sorted $HLA\text{-}G^+$ T cells compared to tTregs and $HLA\text{-}G^-$ cells using NanoString Technologies. (A) Tables present raw data of statistically significantly differentially expressed genes including downregulated (left table) and upregulated (right table) genes in $HLA\text{-}G^+$ T cells compared to tTregs and/or $HLA\text{-}G^-$ T cells. p value threshold < .05, log2 fold change >1.5. (B) $HLA\text{-}G^-$ subset collected as the non-$HLA\text{-}G^+$ fraction following cell isolation using MACS from patients with AD were tested for their suppressive capacity. Representative flow histograms of proliferating live $CD3^+$ responder T cells in the presence of HLA-G-depleted fraction (as suppressor cells) (N=2) tested at increasing ratios (left panel). Percentage of suppression was measured by assessing CPD-labelled responder T cell proliferation at in the presence of α-CD3 stimulation after 5 days of co-culture (right panel). (C) Comparison of the suppressive capacity between $HLA\text{-}G^+$ cells and their HLA-G negative counterparts at the lowest ratios where the $HLA\text{-}G^+$ cells percentages of suppression were most potent.

Supplementary Figure S5. Evaluation of $HLA\text{-}G^+$ phenotype following pre-treatment in sera and the role of IL-35 in inducing $CD4^+HLA\text{-}G^+$ suppressor cells. (A) Assessment of the effect of sera at inducing $HLA\text{-}G^+$ phenotype in cultured $CD4^+$ T cells from HCs following 48hrs of culture in the presence of 25% sera from SC and AD (n=15 per group). (B) Concentrations of IL-35 in sera samples from liver disease patients (SC; n=25 and AD; n=25). (C) Assessment of the effect of IL-35 in driving this phenotype was tested by pre-incubating sera in the presence or absence of α-IL-35 neutralising antibody (10 µg/ml) prior to $CD4^+$ T cell exposure to sera from HC or SC (n=3 and n=4, respectively) (D) Sera-induced-HLA-G expressing $CD4^+$ T cells that resulted from sera-conditioning in the presence or absence of IL-35 blockade were tested for their effect on proliferating healthy control PBMCs (n=7). (E) Proportions of sera-induced HLA-

G expressing $CD4^+$ T cells following culture in the presence of sera from SC (n=4) or AD (n=5) patients in the presence or absence of α-IL-10 neutralising antibody (1 μg/ml). Mann-Whitney test for two group comparison and Wilcoxon-matched-pairs signed rank test was used for all paired non-parametric tests. Data are presented as median values with IQR. ns; no significance.

Supplementary Figure S6. Functional investigation of the capacity of HLA-G^+ cells to suppress proliferation in healthy allogeneic PBMCs in the presence of blocking antibodies. (A) Pre-conditioned $CD4^+$ T cells in HC sera tested for their capacity to suppress PBMC proliferation in the absence or presence of CTLA-4 blockade. Representative histograms of proliferating healthy PBMCs in the absence or presence of α-CTLA-4 (left panel). The effect of blocking CTLA-4 in proliferation assays were tested in 6 independent experiments (right panel). (B) Role of HLA-G (left panel) and IL-35 (right panel) blockade in mediating the suppressive capacity of HLA-G-expressing cells. Co-cultured PBMCs with HLA-G expressing cells [generated through preconditioning in sera from AD (n=8) or HC (n=7)] were assessed for their effect on the proliferative capacity of healthy PBMCs in the presence of neutralising antibody against HLA-G and IL-35 (used at 10 μg/ml). (C) Profile of secreted cytokines within the Th17 pathways assessed after blockade of CTLA-4 (top panels) or IL-35 (bottom panels). Wilcoxon-matched-pairs signed rank test was used for all paired non-parametric tests. ns; no significance.

Supplementary Figure S1

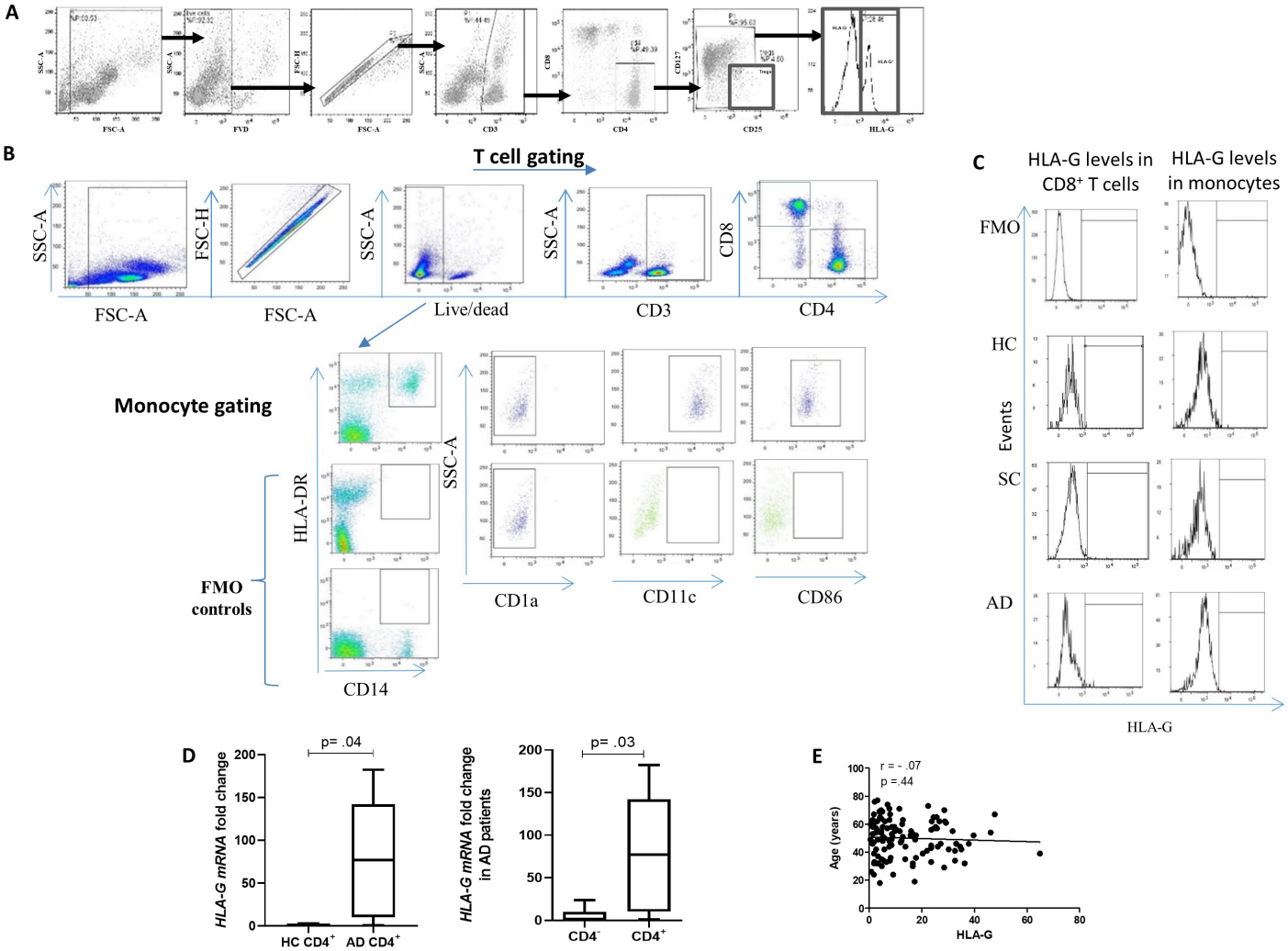

Supplementary Figure S2

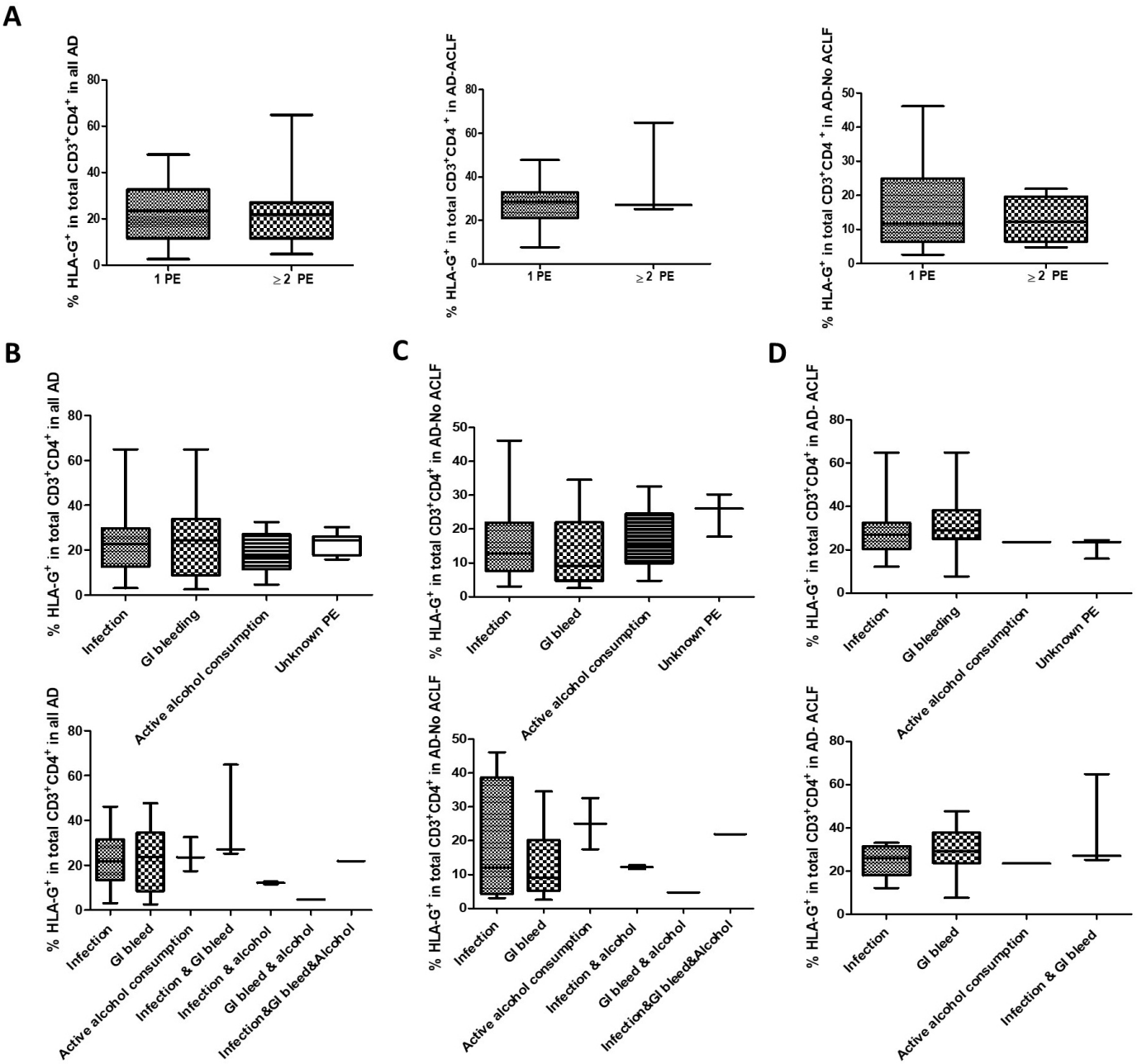

Supplementary Figure S3

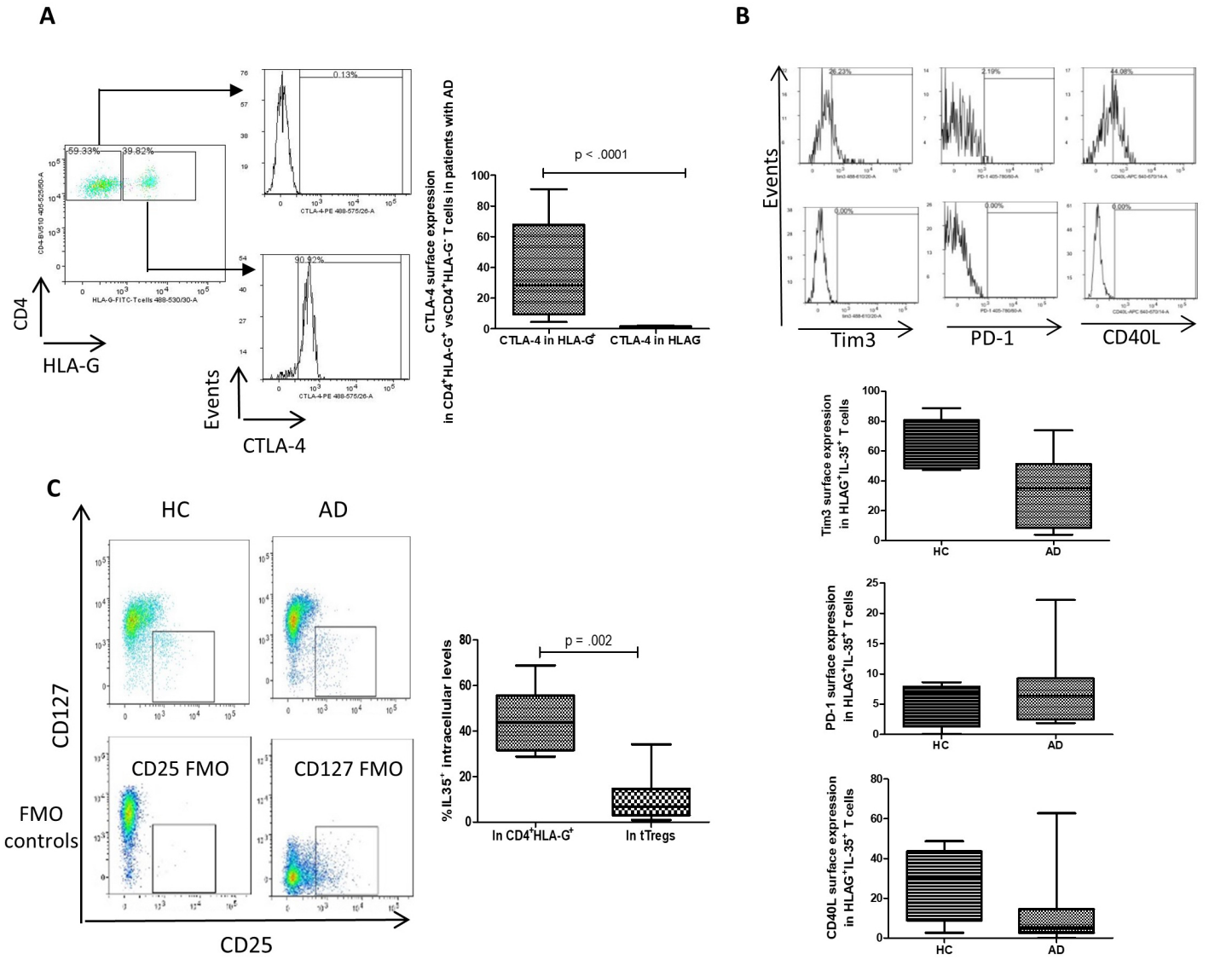

Supplementary Figure S4

A

Down-regulated differentially expressed (DE) genes

HLA-G⁺ T cells vs Tregs			HLA-G⁺ vs HLA-G⁻ T cells			Common DE genes in: HLA-G⁺ vs Tregs			HLA-G⁺ vs HLA-G⁻ T cells		
Gene name	Log2 fold change	P-value	Gene name	Log2 fold change	P-value	Gene name	Log2 fold change	P-value	Log2 fold change	P-value	
FOXP3	-7.79	4.73E-05	MLLT3	-4.64	0.00018	TIGIT	-5.02	0.000423	-2.25	0.0125	
FCRL3	-6.53	8.67E-05	SKIL	-4.62	0.00055	TNFSF4	-4.61	0.00114	-3.58	0.00339	
CXCR6	-5.19	0.00361	PIK3R2	-4.52	2.40E-05	GBP3	-4.47	0.000308	-4.73	0.00018	
EZH2	-4.13	0.00189	DVL2	-4.39	0.00025	SNCA	-3.88	0.000195	-3.61	0.00116	
IL2RA	-4.09	0.00362	POLR3H	-4.38	0.0003	HMGB1	-3.84	0.000561	-4.69	0.00024	
CTLA4	-3.4	0.00335	MDM2	-4.3	0.00059	NFATC1	-3.56	0.00106	-4.92	0.00032	
CD27	-2.42	0.0208	ELAVL1	-4.14	0.00063	RPS6KA5	-3.32	0.00802	-3.54	0.00807	
CASP3	-2.37	0.0342	WNT10B	-4.14	0.00136	IL18R1	-3.22	0.00235	-3.45	0.00133	
RIPK3	-2.3	0.0344	ADORA2A	-4	0.00037	TAB1	-3.16	0.000611	-3.17	0.0001	
ATP6V0A1	-2.13	0.0224	SPPL2B	-3.94	0.00074	NUDT1	-3.04	0.000661	-2.04	0.00161	
FAS	-2.1	0.0209	POLR3D	-3.82	5.67E-05	SOCS5	-2.95	0.00164	-4.18	0.00014	
CD59	-2.08	0.0221	SMAD5	-3.74	0.003	USP21	-2.82	0.00802	-2.93	0.00826	
S1PR4	-2.03	0.0437	LRR1	-3.67	0.0008	TAB3	-2.8	0.000242	-2.75	0.00198	
TRAF3	-1.99	0.0283	PRMT5	-3.66	0.0007	TRAF6	-2.8	0.0055	-3.35	0.00515	
TRAF1	-1.85	0.0162	TRIM68	-3.63	0.00084	CGAS	-2.7	0.0054	-2.64	0.00504	
POLR1D	-1.82	0.0391	TNFRSF13C	-3.54	0.0016	STRADB	-2.64	0.00581	-3.77	0.0002	
RB1	-1.82	0.0132	BAD	-3.5	0.00048	ATG4B	-2.55	0.000377	-2.6	0.00058	
BCL2L1	-1.81	0.0215	LTA	-3.44	0.00084	NPRL2	-2.55	0.00722	-3.34	0.00403	
NF1	-1.55	0.00761	PANX1	-3.3	0.00365	TRIM26	-2.5	0.00902	-2.2	0.0285	
AP1S1	-1.54	0.0203	SOD1	-2.86	0.00418	IL21R	-2.45	0.0154	-2.61	0.0129	
TRIM21	-1.51	0.027	TELO2	-2.64	0.00886	TBK1	-2.44	0.00544	-1.88	0.0278	
			CDK8	-2.56	0.0256	ACP5	-2.26	0.00536	-1.67	0.00567	
			APC	-2.53	0.0176	CTPS1	-2.18	0.000193	-2.62	0.00013	
			RRAS2	-2.3	0.0423	IMPDH2	-2.07	0.00811	-3.56	0.00067	
			STK26	-2.23	0.0145	CARD8	-2.02	0.0163	-2.49	0.0112	
			CCR7	-1.78	0.0157	GHDC	-1.97	0.00251	-2.45	0.0022	
			MAPK11	-1.67	0.00246	IKBKB	-1.93	0.0016	-2.36	0.00217	
			DNMT3A	-1.65	0.0493	MAP3K14	-1.87	0.0247	-1.73	0.0351	
						MTOR	-1.85	0.0268	-2.14	0.022	
						NKIRAS2	-1.75	0.0314	-1.74	0.0338	
						GCLC	-1.7	0.0103	-1.69	0.0186	
						NOTCH1	-1.7	0.0194	-2.32	0.00178	
						CAMK2G	-1.63	0.0453	-1.86	0.0382	
						BRWD1	-1.62	0.0362	-1.93	0.0216	
						TICAM1	-1.58	0.0139	-2	0.00651	
						TRAF2	-1.56	0.0241	-1.84	0.0149	

Up-regulated differentially expressed (DE) genes

HLA-G⁺ T cells vs Tregs			HLA-G⁺ vs HLA-G⁻ T cells			Common DE genes in: HLA-G⁺ vs Tregs			HLA-G⁺ vs HLA-G⁻ T cells		
Gene name	Log2 fold change	P-value	Gene name	Log2 fold change	P-value	Gene name	Log2 fold change	P-value	Log2 fold change	P-value	
LTB	1.53	0.0162	CTSC	1.53	0.00034	ALOX5	2.02	0.0433	2.38	0.00231	
SOCS3	1.69	0.00769	AHR	1.64	0.0216	SIRT1	2.66	0.00427	2.6	0.00516	
TXNIP	1.7	0.0107	HIST1H4H	1.69	0.00178	S100A8	2.59	0.0428	3.8	0.0129	
IL7R	3.38	0.00106	TNFRSF1A	1.76	0.0126	ANXA1	2.51	0.00531	2.36	0.00167	
			CD52	1.78	0.00202	S100A9	2.45	0.0409	3.62	0.0137	
			HIST1H2BK	1.84	0.01	SPI1	2.35	0.0276	3.61	0.00777	
			HIST1H2BF	1.94	0.0129	NFKBIA	2.27	0.00108	1.79	0.00402	
			SLC7A5	1.95	0.0441	TLR2	2.25	0.0369	3.33	0.00772	
			TNFRSF1B	1.96	0.00032	TYROBP	2.23	0.0247	3.29	0.0104	
			CFP	2.34	0.0165	IFITM3	2.14	0.00387	3.23	0.00081	
			NKG7	2.43	0.0437	IFI30	2.12	0.0262	3.24	0.00953	
			FCGR3A/B	2.83	0.0209	CYBB	2.1	0.042	3.31	0.0102	
			FCN1	2.85	0.0229	CXCL8	2.09	0.041	3.25	0.0118	
			CXCL2	3.18	0.043	IFNGR1	1.94	0.02	2.41	0.00347	
			CD68	3.22	0.0143	GRN	1.89	0.0238	2.9	0.00717	
			CD14	3.31	0.0197	HLA-DRA	1.76	0.0117	3.18	0.00647	
			S100A12	3.75	0.0171	HLA-DRB1	1.73	0.0347	3.52	0.00438	
			F13A1	3.8	0.0134	CD74	1.69	0.00377	2.99	0.00172	
						GSTP1	1.62	0.0128	2.26	0.00286	
						HLA-B	1.54	0.00344	1.65	0.00248	
						ITGB2	1.52	0.0091	2.16	0.00287	
						E2F4	1.5	0.00903	1.63	0.00636	

B

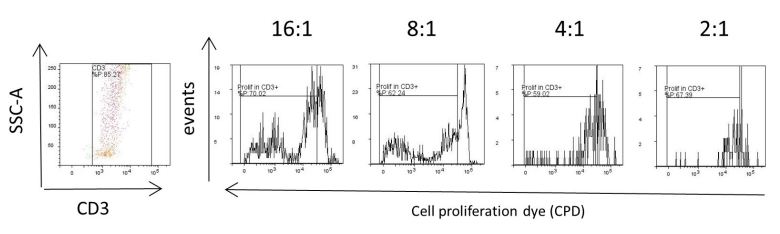

C

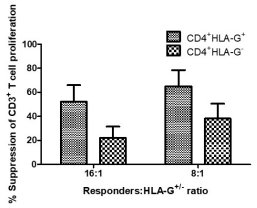

Supplementary Figure S5

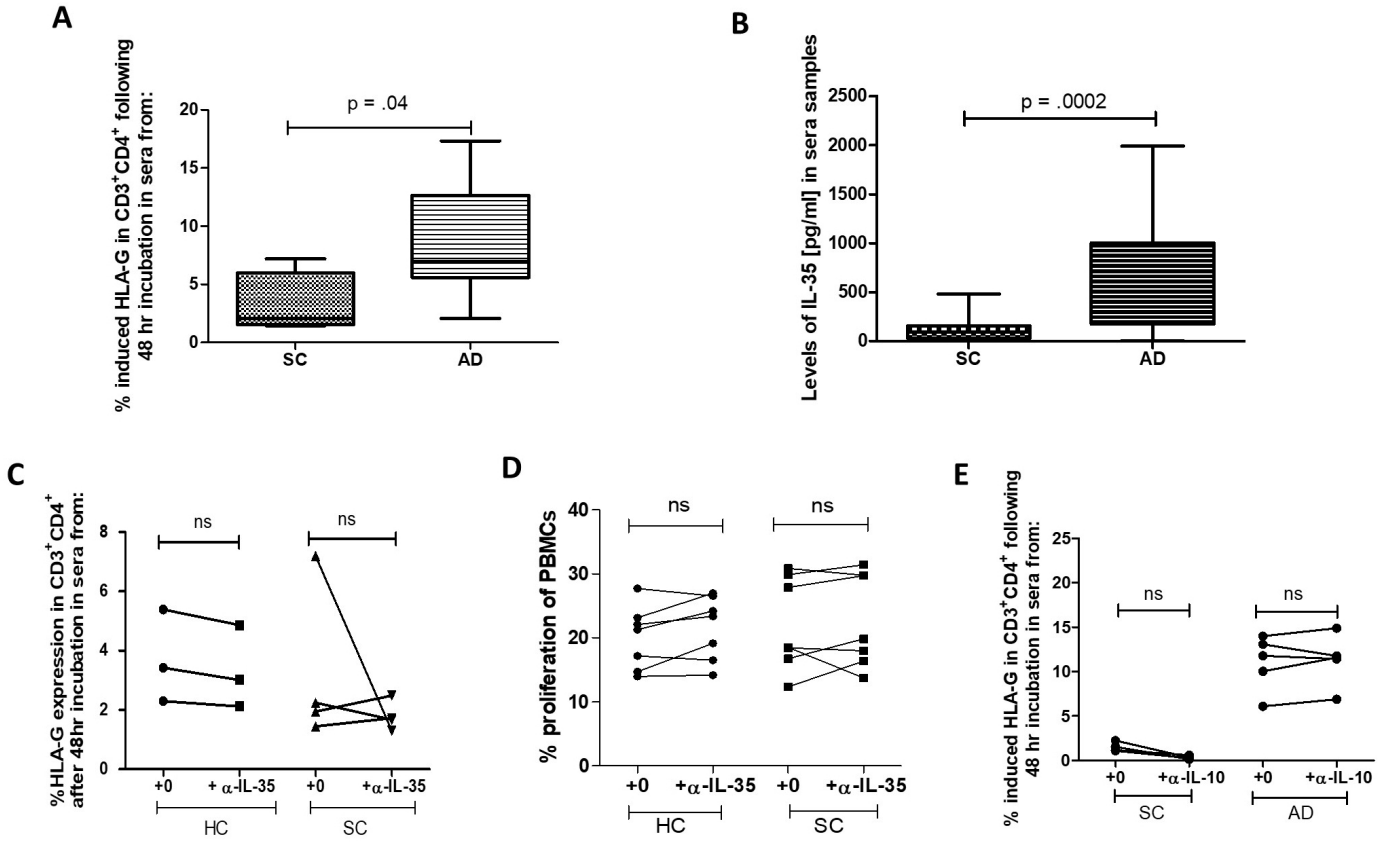
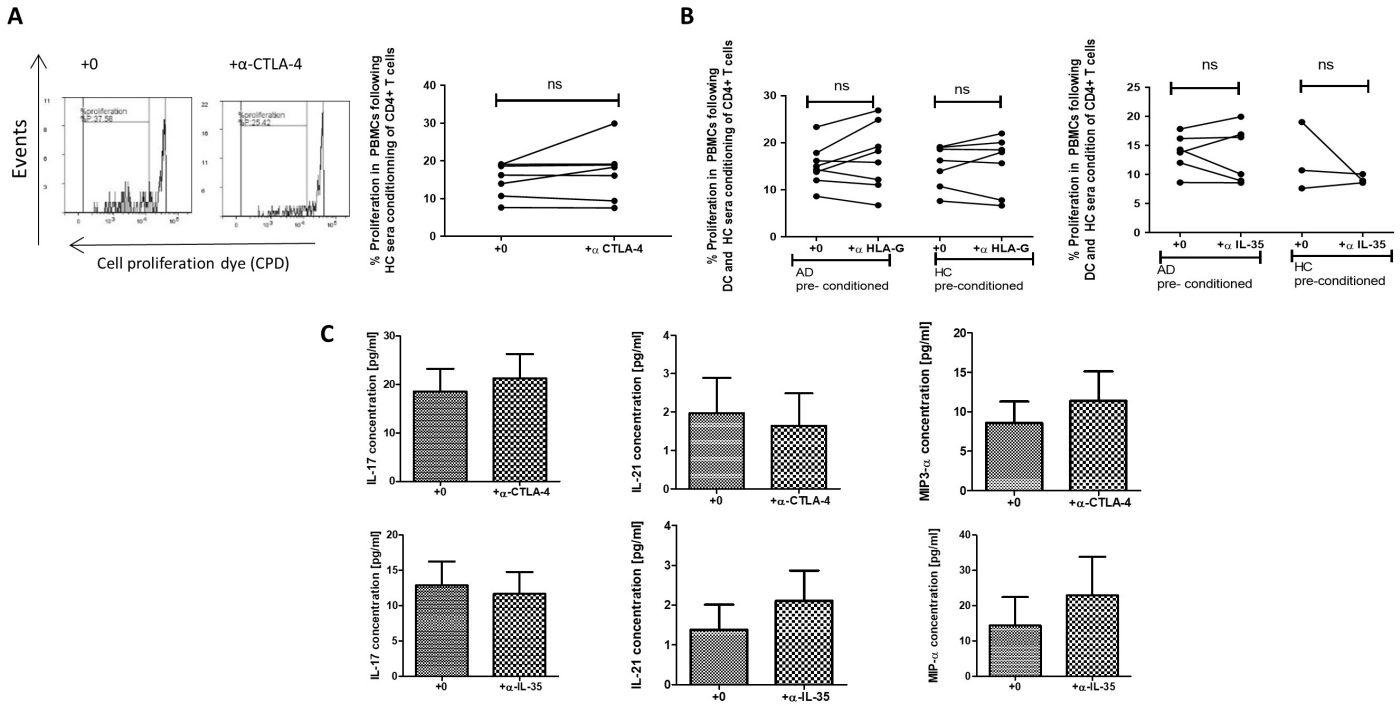
Supplementary Figure S6